DISSERTATION

# TERMINAL FALL VELOCITY OF PARTICLES OF IRREGULAR SHAPES AS AFFECTED BY SURFACE AREA

Submitted by

George R. Alger

In partial fulfillment of the requirements

for the Degree of Doctor of Philosophy

Colorado State University

Fort Collins, Colorado

July 1964

COLORADO STATE UNIVERSITY

July 1964

WE HEREBY RECOMMEND THAT THE DISSERTATION PREPARED UNDER OUR SUPERVISION BY George R. Alger

ENTITLED TERMINAL FALL VELOCITY OF PARTICLES OF IRREGULAR SHAPES AS AFFECTED BY SURFACE AREA

BE ACCEPTED AS FULFILLING THIS PART OF THE REQUIREMENTS FOR THE DEGREE OF DOCTOR OF PHILOSOPHY

Committee on Graduate Work

D. B. Simons
Major Professor

S. Karaki

E. V. Richardson

Roberta F. Johnson

Maurice L. Albertson

Head of Department

Examination Satisfactory

Committee on Final Examination

E. V. Richardson

S. Karaki

Roberta F. Johnson

D. B. Simons
Chairman

Permission to publish this report or any part of it must be obtained from the Dean of the Graduate School.

## ABSTRACT OF DISSERTATION

## TERMINAL FALL VELOCITY OF PARTICLES OF IRREGULAR SHAPES AS AFFECTED BY SURFACE AREA

The objective of this research is to study the effect of surface area on terminal fall velocity of particles and objects of irregular shapes. An auxilliary study was also made in a qualitative manner on the effect of various concentrations of neutrally buoyant fine material on the fall velocity of spheres. The results of this auxilliary study are given in Appendix (B). It is expected that these investigations will lead to further research in areas related to these topics.

Various shapes of gravel-sized particles were studied. The terminal fall velocities were obtained by repeatedly dropping the same particles in fluids with different viscosities. A photographic technique was used to determine these terminal velocities. A new shape parameter was developed and the variation of drag coefficient with Reynolds number using this new parameter is given. This $C_d$ versus Re relation leads to the possibility of a model law for the irregular shapes with the new shape parameter as the third variable. A limited verification is given for several selected machined shapes and for ordinary concrete test cylinders. The model verification was accomplished by dropping larger scale particles in water and measuring terminal fall velocity using a specially constructed large scale speedometer.

Plastic (Vestyron) particles were used to form a neutrally buoyant suspension in salt water. A small plastic sphere was dropped through various concentrations of this suspension and the fall velocity was determined with a stop watch. The results indicate the need to study the electrochemical properties of the suspended fine material as they appear to affect the fall velocity of the larger particle. The writer believes from the results obtained that the consideration of the Zeta potential of the fine material would ultimately lead to a better description of the apparent viscosity effects when used in conjunction with existing theories.

George R. Alger
Civil Engineering Department
Colorado State University
July 1964

ACKNOWLEDGEMENTS

The writer wishes to express his sincere appreciation to Daryl B. Simons, the writer's major professor, and to H. P. Guy and E. V. Richardson of the United States Geological Survey for their valuable comments, suggestions and encouragement.

Acknowledgement is also due other members of the United States Geological Survey for their support and suggestions during the course of this work.

The writer wishes also to express his gratitude to the United States Geological Survey for their financial support and to the other members of this committee, John W. N. Fead, Maurice L. Albertson, Susumu Karaki, and Roberta F. Johnson.

TABLE OF CONTENTS

TABLE OF CONTENTS - continued

LIST OF FIGURES

LIST OF FIGURES - continued

# TABLES

# DEFINITION OF SYMBOLS

| Symbol | |
|---|---|
| A | Cross sectional area ($cm^2$) |
| a | Maximum dimension of a particle (cm) |
| a' | Acceleration ($cm/sec^2$) |
| b | Intermediate dimension of a particle (cm) |
| c | Minimum dimension of a particle (cm) |
| $C_d$ | Drag coefficient |
| $C_{do}$ | Drag coefficient of original particle |
| $C_{dl}$ | Drag coefficient of modified particle |
| $d_A$ | Surface diameter (Diameter of a sphere having the same surface area as that of the particle) (cm) |
| $d_n$ | Nominal diameter (Diameter of a sphere which has the same volume as that of the particle) (cm) |
| F | Submerged weight of the particle (gms) |
| g | Acceleration owing to gravity (980.7 $cm/sec^2$) |
| K | $\frac{2(\rho_s - \rho_f)\, g}{\rho_f}$ $(cm/sec^2)$ |
| M | Mass (gms) |
| Re | Reynolds number $\left(\frac{V\ell}{\nu}\right)$ |
| $Re_o$ | Reynolds number of original particle $\left(\frac{V\ell_o}{\nu}\right)$ |
| $Re_l$ | Reynolds number of modified particle $\left(\frac{V\ell_l}{\nu}\right)$ |
| S | Surface area ($cm^2$) |

| Symbol | |
|---|---|
| Sx | Standard deviation $\sqrt{\frac{\sum x^2 - \frac{\left(\sum x\right)^2}{n}}{\eta - 1}}$ |
| S. F. | Shape factor $\frac{c}{\sqrt{ab}}$ |
| V | Terminal fall velocity (cm/sec) |
| V' | Terminal velocity in a clear liquid containing no fine material (cm/sec) |
| Vc | Terminal velocity in a solution containing a certain concentration of neutrally buoyant fine material (cm/sec) |
| ~~V~~ | Volume ($cm^3$) |
| $\mu$ | Dynamic viscosity $\frac{gm}{cm/sec}$ |
| $\nu$ | Kinematic viscosity ($cm^2/sec$) |
| Z | Change in drag coefficient from original particle to the modified particle |
| Z. P. | Zeta potential (millivolts) |
| $\rho_f$ | Mass density of fluid $\frac{gm\text{-}sec^2}{(cm^4)}$ |
| $\rho_p$ | Mass density of particle $\frac{gm\text{-}sec^2}{(cm^4)}$ |
| $\rho_w$ | Mass density of water $\frac{gm\text{-}sec^2}{(cm^4)}$ |

## DEFINITION OF TERMS

Apparent viscosity - viscosity of a dispersion of fine solid material in water

Cation exchange capacity (C. E. C.) - amount of exchangeable ions adsorbed per unit mass (milli. equiv./100 grams)

Nominal diameter ($d_n$) - the diameter of a sphere which has the same volume as the particle

Sedimentation diameter - diameter of a sphere that has the same specific gravity and has the same terminal fall velocity as the particle in the same sedimentation fluid

Surface diameter ($d_A$) - diameter of a sphere which has the same surface area as the particle

Terminal fall velocity - constant velocity that a particle will attain when falling alone in a quiescent fluid of infinite extent. (Velocity at which the net gravitational force is equal to the resistance to fall).

Zeta potential (Z. P.) - energy required to bring a unit positive charge from infinity to the immobile layer (Milli. volts)

# CHAPTER I

## INTRODUCTION

The demand for domestic, commercial, and agricultural water supplies places more emphasis on the physics and mechanics of water storage and conveyance. The problems involved are numerous and often complex. One such problem area is that of transport and deposition of sediment which has been of interest to the United States Geological Survey at Colorado State University for several years. Although much progress has been made, many of the variables and parameters governing the transport and deposition characteristics of sediment are still in need of research. One important problem, chosen for this study, is that of the terminal fall velocity of irregular gravel-sized sediment particles.

The relationship between drag coefficient ($C_d$) and Reynolds number (Re) for regular shapes which may be expressed in mathematical terms (a sphere, disk, flat plate, etc.) has been studied extensively. These relationships have been summarized in the form of curves which related the coefficient of drag ($C_d$) to the Reynolds number (Re) with a parameter expressing particle shape as a third variable. Consequently the third parameter in the drag coefficient versus Reynolds number relationship is some standard shape that has a mathematical expression for surface area and volume. When one deals with naturally worn sediment particles which are in general irregular in shape, surface area, and surface roughness mathematical expressions are not easily obtained;

however, some characteristic parameter is needed in order to describe each particle as to its behavior in the $(C_d)$ versus (Re) relations. One such parameter that has been customarily employed to express particle shape is the Corey shape factor. This shape factor will be discussed in more detail in the chapter on theoretical analysis.

Much study has been devoted to analysis of raindrops falling through air and to the phenomenon of air bubbles rising through water. The problem of variable density is involved in these studies since the air bubble changes its size with changes in local pressure and the rain drop shape is molded by local resistance and surface energy which in turn is a function of surrounding air density. Thus, the problems involved in these areas are not completely similar to those involved with solid particles, as the motion of the solid particles is governed by shape, while the shape of the raindrop and air bubble is molded by the type of motion.

For solid particles it is apparent that a parameter should be found which would uniquely characterize each sediment particle as to its hydraulic behavior under free fall conditions and that would work well with the usual drag and Reynolds number type of relation.

It also appears that factors such as shape, surface area, and roughness may affect such a parameter to varying degrees. Several studies by various investigators have been devoted to finding such a parameter; however, these have not proven to be completely satisfactory

due to the difficulty of measurement of the various shape parameters as well as large scale scatter of the data.

Another aspect involved in the analysis of sediment transport is that of the effect of various concentrations of fine material in the transportive medium on the fall velocity of the larger particles. This appears to be related to an apparent viscosity effect due to the presence of the fine material. This effect has also been investigated by various researchers, but further attention was given to this problem in the development of this dissertation. This problem study was made as an auxiliary topic and is treated in a qualitative manner in Appendix B.

A. The Problems

(1) What effect does surface area have on the Corey shape factor as used in existing ($C_d$) versus (Re) relationships?

(2) If a significant effect exists what new shape parameter would better describe the ($C_d$) versus (Re) relationship?

(3) What effects do varying concentrations of different sizes of neutrally buoyant fine materials have on the fall velocity of particles?

B. Problem Analysis

The solution of these problems depends on the following conditions:

1. Knowledge of the factors affecting fall velocity.

2. A method of measuring surface area of irregular shapes.

3. The correlation of a shape parameter and surface area parameter to establish ($C_d$) versus (Re) relationship which better describes particle behavior under free fall conditions.

4. A means of forming a neutrally buoyant suspension of fine material in which the affect on fall velocity can be investigated.

C. Scope of the Work

The gravel-sized particles studied ranged in size from a nominal diameter of approximately 2 to 4 centimeters. The larger particles tested for verification of a possible model law ranged in size from 9 to 22 centimeters in nominal diameter. Reynolds numbers varied from approximately 10 to 400,000. The fine material used to form a neutrally buoyant suspension was composed of several sizes of small plastic pellets and spheres.

# CHAPTER II

## REVIEW OF LITERATURE

In order to keep the pertinent reference material separated for the two topics treated in this work, the review is divided into two main sections with a summary:

A. Particle shape and fall velocity.

B. Apparent viscosity.

C. Summary.

### A. Particle Shape and Fall Velocity

One of the earliest scientists interested in fall velocity was Sir George Stokes. Lamb (31) gives Stokes formulation (known as Stokes Law) as $F = 3\pi D\mu V$ for viscous flow conditions where:

F is the longitudinal force exerted by a slowly moving viscous fluid upon a small sphere

D is the diameter of sphere

$\mu$ is the dynamic viscosity

V is the terminal fall velocity

Some years later in 1908, due to problems arising in the ore dressing industry, Richards (8) studied fall velocities of quartz and galena particles and attributed the differences in his results to the difference in specific gravity of the two materials.

In 1934, Zegrzda (16) showed that differences in specific gravity could not account for the results of Richards and pointed to particle shape

as the cause. Zegrzda's plot of $(C_d)$ versus (Re) was broken down into three ranges; streamline or Stokes range, intermediate or transition range, and turbulent range.

Wadell (12), (13), (14) in 1935 regarded sphericity as the parameter to use in expressing shape of a particle. He defined sphericity as the ratio of the surface area of a sphere having the same volume as the particle to the surface area of the particle. However, recognizing the difficulty of measuring irregular surface areas he further proposed to define sphericity as the ratio of the diameter of a circle equal in area to the projected area (obtained when the particle rests on one of its larger faces) to the diameter of the smallest circle circumscribing the projected area. This, however, left the erroneous result of spheres and disks with the same sphericity but having different fall characteristics. Also, this factor did not take into account the thickness of the particle.

In 1938 Heywood (2) suggested a "volume constant" K as a shape parameter defined as

$$K = \frac{\text{Volume of particle}}{d^3}$$

where

d is the diameter of a circle of area equal to the projected area of the particle when placed in its most stable position. He also prepared a nomograph from which fall velocity could be determined if the volume constant K was known.

Krumbein (3) in 1941 demonstrated that fall velocity proved to be an adequate index of the critical velocity required to cause movement of

sediment particles as well as for the quantity of sediment transported per unit time. He also suggested a shape parameter

$$\Omega = \sqrt[3]{\frac{b^2}{a}\,\frac{c}{b}}$$

where

a is the longest axis of the particle

b is the intermediate axis of the particle

c is the shortest axis of the particle

The terms in the above relation proved to be easier to measure than those suggested earlier investigators.

In 1948, Serr (10) proposed the ratio of sedimentation diameter to sieve diameter as a means of expressing shape. Serr concluded from his investigations that shape has little effect on fall velocity for all sand grains less than 0.05 mm in diameter. He also showed that shape has an important influence on the type of motion experienced by a falling particle.

In 1948, McNown, Lee, McPherson, and Enges (5) worked out relations for the influence of boundary proximity on the drag of spheres. From the analysis of Stokes, for small inertial effects, the resistance to motion F was given by

$$F = 3\pi\ u\ V\ d$$

The equation can be modified by the introduction of a coefficient K to include the effect of cylindrical boundary so that

$$F = K\ 3\pi\ u\ V\ d$$

For large Reynolds numbers the resistance to motion is given by

$$F = C_d \rho A \frac{V^2}{2}$$

where

$C_d$ is the coefficient of drag

$\rho$ is the fluid density

A is the cross sectional area of a sphere

The coefficients K and $C_d$ may be related by

$$K = \frac{C_d \, Re}{24}$$

where

Re is the Reynolds number.

An approximate solution for K is given as

$$K = 1 + \frac{9}{4} \frac{d}{D} + \left(\frac{9}{4} \frac{d}{D}\right)^2$$

where

d is the diameter of sphere

D is the diameter of cylinder

At the point where $\frac{d}{D}$ approaches 1, it is assumed that the flow is similar to that between the flat plates and considering continuity, geometry and equilibrium, a second approximation is obtained for K for large diameter ratios.

$$K = \frac{3\sqrt{2}}{8} \left(1 - \frac{d}{D}\right)^{-5/2}$$

Experiments were conducted to check the formulations. For negligible inertia effects, the data substantiated the formulations for $\frac{d}{D}$ less than

0.1. For $\frac{d}{D}$ approaching 1, the results agreed closely for $\frac{d}{D}$ greater than 0.95.

The Reynolds number for which inertial effects become appreciable increases from $Re = 0.2$ for $\frac{d}{D} = 0$ to $Re = 70$ for $\frac{d}{D} = 0.8$ indicating that the magnitude of the viscous force increases more rapidly with $\frac{d}{D}$ than does the inertial force.

A hexagonal pattern was assumed in order to make a typical concentration analysis in which the effective spacing of particles was S. The effective spacing S was related to the concentration C by

$$\frac{d}{S} = \alpha^3 \sqrt{c}$$

where $\alpha = 1.2$ (a constant) for the hexagonal pattern. A nomograph type relation was drawn involving $\frac{d}{S}$, K, $\frac{d}{D}$, and C in percent, from which it is determined that, for a sediment diameter of 0.0001 feet and a concentration of 10 percent, a settling velocity of 33 percent less than that given by Stokes equation would result.

The most widely used parameter for expressing shape is that proposed in 1949 by Corey (1). This expression is

$$S.F. = \frac{c}{\sqrt{ab}}$$

where

S.F. is the shape factor

a is the longest axis of the particle

b is the intermediate axis of the particle

c is the shortest axis of the particle

This factor actually appears to express the degree of flatness of a particle. As noted by Corey and others, particles tend to fall with their maximum projected area normal to the direction of fall and the product ab is an approximation of this area while c accounts for the thickness which was ignored in Wadell's (12), (13), (14) work. However, the degree of angularity and degree of roughness are still not accounted for. The distribution of surface area is also unreal since a disk and a cross of the same thickness and diameter have the same shape factor. Also, spheres and cubes have the same shape factor.

In 1959 Jamil Malaika (4), using a photographic technique developed by McPherson (7) and specially machined metal shapes, concluded that in the "deformation drag zone" the particles are stable in any position (Re less than 0.1), in the "surface drag zone" (Re greater than 0.1 but less than 500) the particles tended to orient with their largest cross section normal to the line of fall, and in the "zone of eddy formation" (Re greater than 500) particle stability was affected by formation of eddies in the wake.

In 1950, McNown and Malaika (6) reviewed the data on metal shapes that Malaika had gathered and independently developed a shape parameter the same as that suggested by Corey. Sieve diameter and sediment diameter were related by a factor K

$$K = \frac{Ws}{W}$$

where

Ws is the fall velocity of a sphere with diameter equal to the nominal diameter of the particle.

W is the fall velocity of the particle.

In 1952 Wilde (15), working with gravel-sized particles, compared the product ab with the actual projected area of the particle. The ratio of projected area to ab was found to average 0.75. A comparison of data for naturally round and sharply angular particles showed poor correlation using the shape factor $\frac{c}{\sqrt{ab}}$ and Wilde reasoned that $\frac{c}{\sqrt{ab}}$ does not take into account the factor of angularity.

He explored the possibility of using a shape parameter equal to the ratio of particle volume to projected area but decided that little advantage would be gained and projected area was more difficult to measure than the terms in $\frac{c}{\sqrt{ab}}$.

In 1953, Schulz (9), while studying size ranges from 0.2 mm to 0.5 mm and using the Corey shape factor, noted the large scatter of his and others' data on the $C_d$ versus Re plot with the Corey shape factor as the third variable. He attributed this scatter to measurement error or to possibly some unknown factor. Schulz's $C_d$ versus Re plots show data for both naturally worn and also angular particles.

The United States Interagency Report No. 12 (11), 1957, gives a relation between $C_d$ and Re for various particles. The net gravitational force acting on a particle is given by

$$F = \left(\frac{\pi}{6}\right) d_n^{\,3} (\rho_s - \rho_f)\, g$$

where

$d_n$ is the nominal diameter

$\rho_s$ is the mass density of particle

$\rho_f$ is the mass density of fluid

$g$ is the acceleration of gravity.

The force $F$ resisting the fall, as given by Newton is

$$F' = C_d\, A\, \rho_f \frac{V^2}{2}$$

$A$ is the cross sectional area of the particle in the direction of motion

$V$ is the terminal fall velocity

$C_d$ is the drag coefficient

when the particle falls at terminal velocity $F = F'$, and

$$C_d = \frac{(\pi / 6\, d_n^{\,3} (\rho_s - \rho_f)\, g}{A\ \rho_f \frac{V^2}{2}}$$

The Reynolds number (Re) is given by

$$Re = \frac{Vd}{\nu}$$

where

$V$ is the velocity

$d$ is a characteristic physical length

$\nu$ is the kinematic viscosity

In order to make a plot of $C_d$ versus Re for irregular shapes, d is taken as $d_n$ and A is calculated from $A = \frac{\pi d_n^2}{4}$ and the shape factor of the particle is S. F. $= \frac{c}{\sqrt{ab}}$ .

B. Apparent Viscosity

Baver (27) gives reference to some of the earlier investigations regarding viscosities of suspensions by Einstein. Einstein proposed the formula $N_s = N_m (1 + 2.5\ \phi)$

where

Ns is the viscosity of the colloidal system

$N_m$ is the viscosity of the dispersion medium

$\phi$ is the volume of the dispersed phase per unit volume of solution.

which indicates that the apparent viscosity of the colloidal system depends on the total volume of the particles and is independent of the degree of dispersion. The particles were assumed spherical and ridged and $\phi$ included any water of hydration.

Yotsukura (25) pointed to some later modifications to the Einstein formulation as proposed by Brinkman, Roscoe, Vand, and Hatschik. Brinkman and Roscoe derived an equation

$$Nr = \frac{1}{(1 - C_v)^{2.5}}$$

where

Nr is the ratio of apparent to fluid viscosity

$C_v$ is the volumetric concentration of solids.

This equation was proposed to be valid for varying size fractions within the same suspension. Roscoe further modified this equation to include concentrations of suspended material in which particles rotate as a spherical clot. For this case

$$Nr = \frac{1}{(1 - 1.35\ C_v)^{2.5}}$$

Later Vand made further modification to include clotting of the particles in the shape of a dumbbell by

$$Nr = \frac{1}{1 + 2.5\ C_v + K\ C_v^{\ 2}}$$

where K was a constant. Hatschik has indicated an equation for volume concentrations of more than 50 percent as

$$Nr = \frac{1}{1 - C_v^{\ 1/3}}$$

All of the above modifications were for suspensions of ridged non-attracting particles.

In 1922 Bingham (28) referred to the coefficient of viscosity as $N = \frac{FS}{V}$ and the coefficient of fluidity as $\phi = \frac{1}{N}$ where

F is the shear force per unit area

V is the velocity of the moving plate

For clay solutions the fluidity is independent of time, agitation, and previous treatment, and the fluidities of suspensions follow the empirical relation

$$\phi = (1 - \frac{b}{c})\, \varphi_1$$

in which

b is the volume concentration of solids

c is the particular value of b for which the fluidity becomes zero (c varies from zero to one)

$\varphi_1$ is the fluidity of the medium

With reference to exchange phenomena, Grim (18), in 1952, stated that the cation exchange property of soils is restricted to the clay fractions. Cation exchange capacity is high for montmorillonite and vermiculite, and low for kaolinite and halloysite. The organic component of some soils also shows a great tendency for high exchange capacity. He also points out that the water adsorbed on the surfaces of the clay mineral particles for some distance outward from the surface is not liquid but is composed of layers of oriented water molecules which do not have the properties of liquid water. This in turn effects the apparent size of an individual particle.

Rogers (21), in 1953, was concerned with viscous properties of drilling muds and noted for these very high concentrations that drilling muds are thixatropic or possess different viscosities for different rates of shear. The montmorillonite minerals possess both base exchange and hydration and ionization affect the viscosity of the solution. A usual order of replacement is given by

H, Ba, Sr, Ca, Mg, K, Na, Li

where the degree of hydration and ionization decreases as the type of salt changes from lithium to hydrogen.

Wood, Granquist, and Krieger (24) in 1955 studied viscosities of dilute clay mineral suspensions. They suggested bentonite suspensions are non-Newtonian and thixatropic and that clay suspensions showed a need for aging (72 hours) before fluidity became stabilized. They suggested also that for concentrations less than or equal to 5 percent the ratio of viscosity of solution to that of water is independent of the temperature and that the viscosity of dilute clay suspensions is governed by the geometry of the particles rather than by specific interactions between particle and solvent or between particle and particle.

Baver (27) in 1956, mentions that in a colloidal solution it is assumed that the particles are hydrated and that friction takes place between the water molecules of the water hull and the dispersion medium. Colloids are divided into two groups, hydrophile and hydrophobe, with respect to their viscous properties. The hydrophilic sol are characterized by high viscosity while the hydrophobic do not possess a viscosity appreciably different from that of their dispersion medium. Clay soils can be classified as occupying an intermediary position. Baver also refers to the equation

$$\frac{Ns}{No} = 1 + 2.5 \frac{\phi}{V - \phi}$$

where

$\frac{Ns}{No}$ is the relative viscosity

V is the total volume of sol

$\phi$ is the effective volume of the dispersed phase.

It is noted that the effects of the amount and nature of the exchangeable cation affects the viscosity of clay soils. Most clay particles possess a negative charge; the magnitude of the charge is known as the Helmholtz double layer. The inner layer is part of the wall of the particle. It migrates with the particle in an electric field and determines the sign of the charge on the particle. The outer layer is of opposite sign and is at a distance of molecular dimensions from the inner layer. The ions of the outer layer are easily replaced by other ions. The possibility of replacement becomes greater the further the ion of the outer layer is removed from the inner layer or in other words, the greater the thickness of the double layer or zeta potential.

In 1958, Norman Street (23) presented a paper on the viscosity of clay suspension and stated that clay suspensions usually exhibit non-Newtonian viscosity. It is often assumed that suspensions of clay minerals behave as plastic fluids, in other words, have a definite yield value that must be exceeded before flow can begin. However, it seems that these solutions can better be described in terms of a mixture of both pseudo-plastic and plastic flow. A reduction of zeta potential and not necessarily of particle charge causes the decreased repulsion at high electrolyte concentrations. The increase in electrolyte concentration decreases the double layer thickness. The viscosity of solution depends

on the type of adsorbed cations on the clay particle. This ranges from high viscosity with Li to low viscosity with Ca.

In 1958, Chakravarti (17) conducted tests on hydrogen kaolinite, B. D. H. kaolin, hydrogen montmorillonite, and akli bentonite. Results showed that by virtue of its higher zeta potential (Z. P.) and hydration, H-montmorillonite clay suspensions behave as a hydrophilic colloid whereas H-kaolinite, possessing a lower Z. P. and lower hydration, behave as a hydrophobic colloid. A plot of results show the viscosity of H-kaolinite increases regularly but slightly, and that of H-montmorillonite increases more or less rapidly with increasing concentration of the suspensions. He included an excellent plot relating viscosity to concentration for various mixtures of kaolinite and montmorillonite.

In 1961, Simons, Richardson, and Haushild (22) worked with aqueous solutions of kaolin and bentonite. The apparent viscosities of aqueous dispersions of kaolin and bentonite are given for dispersions of 0.5, 1, 2, 3, 5, and 10 percent bentonite and 3, 5, and 10 percent kaolin for temperatures ranging from 5 to 45 degrees centigrade with hexametaphosphate as the dispersing agent. The ratio of viscosity of solution to that of water is found to be independent of the temperature for concentrations less than or equal to 5 percent, confirming the findings of Wood, Granquist, and Kreiger (24). It is also noted that the amount and type of dispersant affects the viscosity of a water-clay solution. The specific weight of the sediment-water dispersion in pounds per cubic foot is

given by

$$\gamma = \frac{\gamma_w \gamma_s}{\gamma_s - 1.03 \frac{C}{10^4}}$$

where

C is the concentration in parts per million by weight

$\gamma_w$ is the specific weight of water

$\gamma_s$ is the specific weight of the sediment

They point to the need for a more exact definition of $C_d$ versus Re relation for irregular-shaped sediment particles.

From results of flume studies it appears that the total sediment discharge of a stream cannot be predicted unless the concentration of fine material and its affect on fall velocity are known.

In general, resistance to flow and bed material transport is decreased in the lower regime and increased in the upper regime when fine sediment is applied to the flow. Addition of fine sediment tends to stabilize the bed and streamline bed forms in the lower flow regime. In the upper flow regime, the reduction in fall velocity that results from the addition of fine sediment may change a plane bed flow to a standing wave or antidune flow, and in general tend to change the bed form from a lower stage of development to the next higher one.

Also in 1961, Riddick (20) presented a paper on the design of a device for measuring zeta potential to be used in the engineering field.

The fundamental equation for determining zeta potential of particles of a size comparable to raw water colloids is given as

$$Z.P. = \frac{UV_t 4\pi}{D_t}$$

where

U is the electroporetic velocity of the particle

$V_t$ is the viscosity of the suspending liquid

$D_t$ is the dilectric constant of the suspending liquid.

In 1962, Hubbell and Khalid Al-Shaikh Ali (19) investigated the effect of temperature on the mechanics of flow in alluvial channels. They found that changes in water temperature cause changes in the total bed material concentration, flow resistance, shear, and sometimes the bed form.

The magnitude and direction of these changes were not the same for all flows. When the temperature changes, the viscosity changes and consequently the fall velocities of the bed material also change. Thus the influence of the bed material is altered and the stream adjusts to accommode the change in fall velocity.

C. Summary

Several methods have been proposed for describing particle shape as it affects the fall velocity of a particle. A parameter which would include all the properties affecting fall velocity of a particle may be a combination of several elements; volume, surface area, roughness,

angularity and flatness. Under certain circumstances roughness and angularity may be difficult to distinguish from one another. It is also conceivable that particles of the same fixed roughness, volume, angularity and flatness would be difficult to differentiate with regard to surface area. One significant property of the well rounded sediment particle which is still in need of further investigation is that of surface area.

At present the most commonly used shape parameter $\frac{c}{\sqrt{ab}}$ (Corey shape factor) is one which considers apparently only the flatness of a particle. This parameter has primarily been accepted because of the relative ease of measurement of the terms in the parameter. However, graphs of $C_d$ versus Re using this parameter as the third variable show a large amount of scatter, pointing to the need for a closer look at the other possible properties of particles. Surface area has been considered as affecting fall velocity of a particle; however, the surface area of an irregular shape has proved to be quite difficult to measure.

The literature also shows that the fluid properties (viscosity and density) and bed-material transport are affected by additions of fine sediment. Bed forms can also be modified by changes in the amount and kind of fine material concentration. Investigations have also shown that apparent viscosity due to concentration of fine material in the flow can materially affect the fall velocity of individual particles and that the mechanics of the condition are not completely understood.

# CHAPTER III

# THEORETICAL ANALYSIS

This section is intended to discuss the theory relative to the dynamics of a freely falling particle in a quiescent fluid and the approach used to investigate surface area as it affects a shape parameter and fall velocity. The fundamental concepts used are also reviewed.

## A. FUNDAMENTAL CONCEPTS

Certain assumptions are generally made in order to develop the relationships among forces acting on solid, freely falling objects. The fluid is assumed to have uniform density and viscosity and the falling particle is assumed to have reached terminal velocity. Under these conditions it is possible to equate the net submerged weight of the particle to the resistance to fall. The relationship for resistance or drag is dependent on the Reynolds number which in turn relates the inertial forces to the viscous forces and provides an index to laminar and turbulent flow.

The total resistance to fall or drag force is composed of two basic components, pressure and shear. The shear component is caused by tangential shear along the particle boundary while the pressure component is caused by the pressure exerted by the fluid normal to the particle boundary. All fluid resistance can be divided into one or a combination of these two components. The shape or form of an object and its orientation to the flow greatly influence the role of pressure and shear in any

given situation (26).

By making use of the Reynolds number (ratio of inertial to viscous forces) it is possible to describe three regions of flow as indicated in the drag-Reynolds number relations. At very small Reynolds numbers (less than 0.5) the flow about a submerged object is laminar and the shape of the object is of secondary importance in relation to the drag. Under these conditions the viscous forces predominate and fluid shear is of primary importance. Henceforth, this region will be referred to as Stokes region named after the man who derived a mathematical solution for purely laminar flow. This solution (known as Stokes Law) is $F = 3\pi\mu Vd$ and the plot of $C_d$ versus $Re$ is a straight line and $C_d = \frac{24}{Re}$. In this region shear contributes 2/3 and pressure 1/3 of the total drag.

As the Reynolds number is increased, the pressure forces contribute more and more to the total drag. The degree of influence of the pressure depends on particle shape, orientation and Reynolds number. This region is referred to as the transition region. The shape of the particle determines the path taken by the fluid and a zone of separation begins to form on the downstream portion of the particle.

At larger Reynolds numbers the inertial effects predominate and the drag coefficient can be regarded as independent of the Reynolds number. This will be referred to as the inertial region. A separation zone is formed and a large reduction in pressure occurs in the wake downstream from the particle. The nature of the separation zone and

the vortices which occur within it, depends on the shape, orientation and Reynolds number. The forces caused by the pressure are of predominat importance in this range of Reynolds numbers.

## B. FLOW PATTERNS

The flow patterns which may occur and the resultant particle motion are dependent on several phenomena of fluid flow past submerged objects. The fundamentals of these phenomena are described below.

### 1. Separation

As the Reynolds number increases the inertial effects become more predominant and the phenomenon of separation occurs.

Fixed zones of separation are associated with angular shapes. A disk (for example) with its circular face normal to the approaching flow will have a separation zone at the circumferential edge of the disk and it will remain there regardless of the fluid or flow characteristics.

For the situation of the gradually expanding boundary the point of separation occurs where $\frac{dv}{dy} = 0$ on the boundary. This separation is characterized by a reversed flow near the boundary. The location of this point varies depending on particle geometry and flow conditions. If the flow near the boundary is laminar the velocity gradient $\frac{dv}{dy}$ near the boundary is relatively small and the particle boundary does not need to expand to any great extent before separation will occur. However, if the boundary layer is turbulent the mixing is much greater

and the velocity distribution is more nearly uniform. The change from this more nearly uniform distribution to zero velocity at the boundary makes $\frac{dv}{dy}$ much larger and thus the boundary may expand from the flow to a greater extent before separation will occur. This point of separation has great influence on the magnitude and distribution of the shear and pressure. A point of separation well forward on the body will have the effect of reducing shear and increasing pressure and a point of separation well downstream on the body will have the reverse effect. Although the location of the point of separation will remain in a fixed position for an angular boundary, the point will shift upstream around the boundary for a surface of slight curvature as the Reynolds number is increased until the flow near the boundary becomes turbulent, at which time it will suddenly shift downstream.

2. Vortex Formation

Separation is accompanied by the formation of vortices. As the separation zone develops vortices are formed at the trailing edge of the particle. In the case of a sphere (26) or disk (35) a vortex ring may be formed. In the case of long cylinders a pair of vortex sheets may form. These are stable at small Reynolds numbers but "break off" at larger Reynolds numbers and new sets alternately form at the two edges. Investigation of a circular cylinder (26) shows the pressure drag gradually increases from 1/3 the total at small Reynolds numbers to about 1/2 when vortices begin to form. Beyond this point the contribution of pressure

jumps to about 75 percent of the total drag when the alternating system of vortices has been formed. Karman derived a theoretical relationship for such a system of well established vortices in terms of the longitudinal spacing $\ell$ and the transverse spacing b. The frequency f of the alternate shedding is given by $f = \frac{Vv}{\ell}$ where Vv is the velocity of the vortex street relative to the cylinder (26).

The alternate shedding of vortices downstream creates corresponding fluctuations in pressure and consequently alternating transverse thrusts on the particle. At much higher Reynolds numbers the vortices appear to break down and blend into the flow as random turbulence.

3. Circulation

Circulation $\Gamma$ is defined as the line integral around a closed curve fixed in the flow. An element of circulation $d\Gamma$ is defined as the product of the velocity component tangent to the curve and the element ds of the closed curve or

$$\Gamma = \oint V_t \, ds$$

If a submerged object is rotated the additional motion gives rise to the phenomenon of circulation. Side thrusts may develop due to this rotation which has been termed the Magnus affect after its discoverer. It has been shown (30) that net circulation about a symmetrical object is zero since the vorticity shed at the top and bottom is the same but of opposite sign. However, if the object is not symmetrical, different

amounts of vorticity are shed from the top and bottom and as a result, a circulation is produced around any contour surrounding body. This phenomenon in turn affects the local pressure distribution around the body.

## C. TYPES OF PARTICLE MOTION

The motion of an individual particle in free fall is stable for very small Reynolds numbers. As the role of the inertial effects becomes greater, however, this stable orientation no longer persists and particle motion will be influenced by the phenomena described in the section on flow patterns. As soon as separation occurs vortices begin to form. These are seldom formed symmetrically about a three dimensional object depending to a great extent on particle shape and orientation to the flow.

Consider for example a thin flat rectangular shape falling through a viscous fluid with its major cross sectional area perpendicular to the direction of fall. At some value of the Reynolds number the vortices that have developed at the edges of the rectangle will release in a regular alternating pattern. The vortices formed at the ends will be effected by those formed on the sides and in the extreme corners of the rectangle a somewhat superimposed result will occur. Since these vortices affect the pressure distribution a resultant alternating force will occur with some eccentricity from the center of gravity, which in turn will impart a torque to the particle (see sketch).

As the particle is tipped slightly to the direction of fall the resultant shear will be directed along the inclined particle and a component of submerged weight will act along the opposite direction with the magnitude of the weight component increasing with increased inclination of the particle.

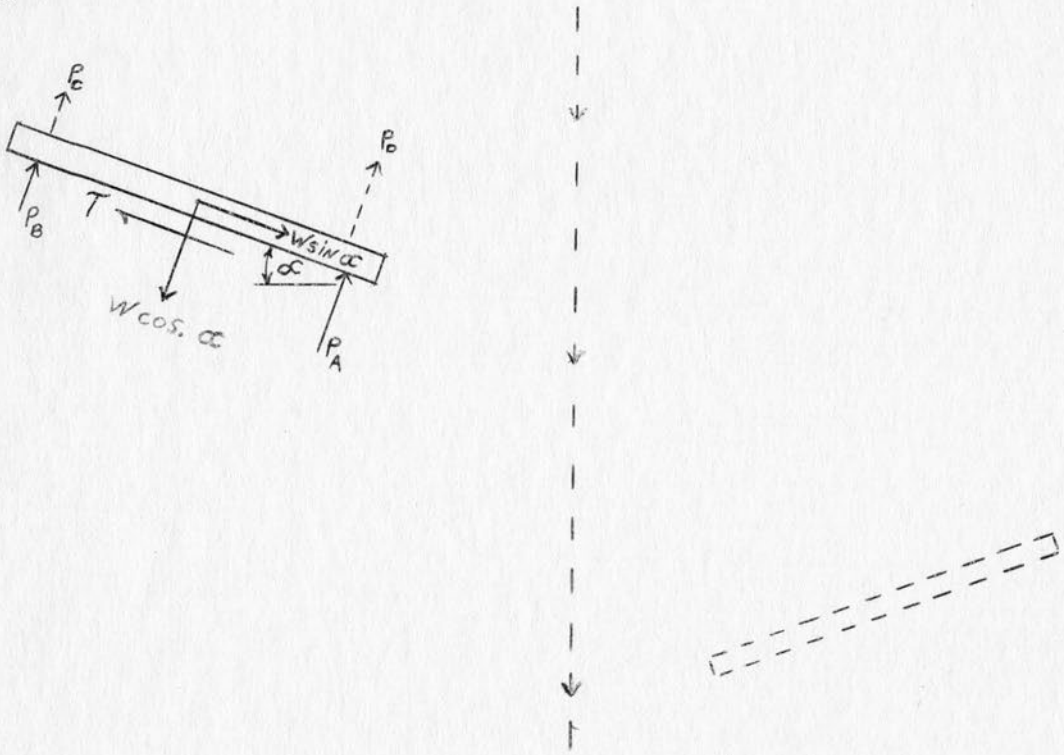


Since the elements of pressure and the other component of the submerged weight act only normal to the surface of the inclined shape there is an unbalanced thrust tending to make the particle slide back towards its original fall centerline as the particle inclination is increased.

As the next vortex system is shed from the opposite end of the particle the reverse process is observed and the mass center of the object is shifted to the opposite side of the fall centerline and the entire process repeated over and over.

At the same time any net circulation present will modify the shear and pressure distribution which in turn will alter the thrust and torque on the particle. Initial local instabilities in the fluid as well as the release mechanism will also influence this behavior. Thus it is seen that particle motion during the formation of vortices may be a sliding, tipping or rotating motion or some combination of these. The net thrust and net torque exerted on the particle will be the integral result of the influence of these motions on the shear and pressure distribution surrounding the particle. The schematic drawing shows the relationship of forces at a certain angle of inclination of the particle. Qualitatively there is a decrease in pressure from A to B and a further decrease from C to D. The greatest pressure reduction occurs from A to D which augments the vortex formation there. The particle itself is experiencing constant periodic changes in velocity as it moves from point to point through the liquid and a summation of forces at any instant is a force equal to the product of particle mass and acceleration. As one applies the above considerations to other shapes it is apparent that the relative order of the magnitude of the respective forces will be altered.

## D. SURFACE AREA AND SHAPE FACTOR

The hydraulic behavior of freely falling solid particles in a viscous fluid may be characterized by two extremes in shape, that of a sphere and that of a thin flat particle. A consideration of these shapes should furnish some information about other intermediate shapes.

With reference to the thin flat particle of Fig. 1 and of surface area S, volume $\forall$, and thickness c, the value of the Corey shape factor is

$$S.F. = \frac{c}{\sqrt{ab}}$$

For purposes of illustration, remove the portion X such that the length o p q = o r q, then the surface area removed is equal to 2S' if S' is the surface area of one side of X. The volume removed is cS' where C represents the average thickness. Since the values of a, b, and c have not changed, the shape factor remained constant. It is now necessary to determine the effect of removing the portion X on the $C_d$ versus Re relation without changing the shape factor (S.F.).

Making use of the drag equation of the form

$$C_d = \frac{\forall \left(\rho_s - \rho_f\right) g}{A \ \rho_f \ \frac{V^2}{2}} = \frac{K \forall}{A \ V^2} \qquad (3.1)$$

where

$\forall$ is the particle volume

A is the cross sectional area

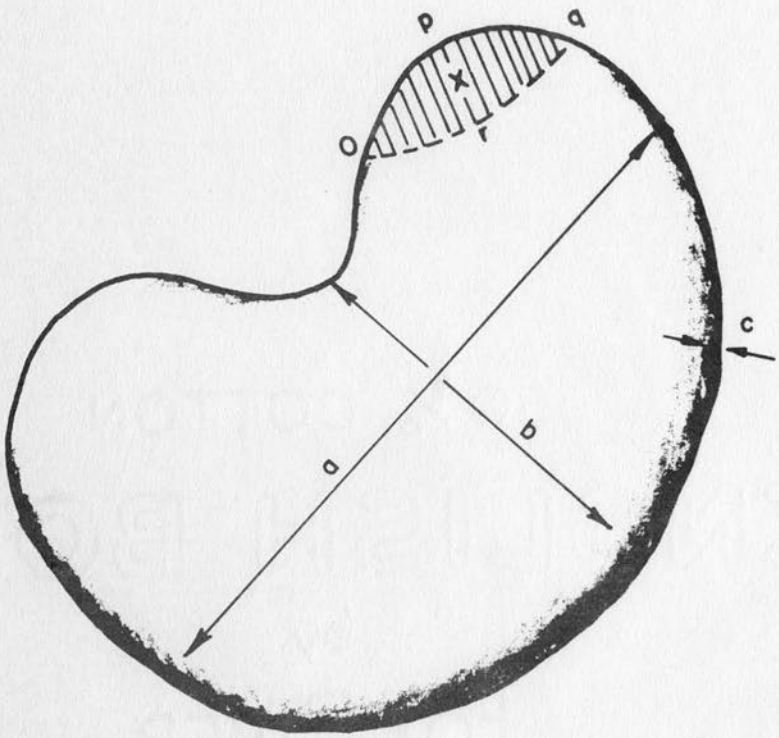


FIG 1 TYPICAL IRREGULAR – SHAPED PARTICLE

$$K \text{ is } \frac{2\left(\rho_s - \rho_f\right) g}{\rho_f}$$

and the region of application is considered outside Stokes range one sees that the coefficient of drag of the original particle $C_{do}$ is

1. decreased by a decrease in ~~V~~
2. increased by a decrease in A
3. increased by a decrease in V

when the portion X is removed.

If one assumes that the area A in the drag equation is that area exposed to the direction of fall and that the particle will fall with its maximum projected area normal to the direction of fall, A is then approximately equal to

$$\frac{(S - cx')}{2}$$

where $x'$ is the circumference of the particle. Then for the original particle

$$C_{do} = \frac{c\,(S - cx')\,K}{(S - cx')\,V_o^2} = \frac{Kc}{V_o^2} \qquad (3.2)$$

where $V_o$ is the terminal fall velocity of the original particle.

For the particle with the portion X removed, the coefficient of drag $C_{d1}$ is

$$C_{d1} = \frac{K\left[\frac{c}{2}(S - cx') - cS'\right]}{\left[\frac{(S - cx')}{2} - S'\right]V_1^2} = \frac{Kc}{V_1^2} \qquad (3.3)$$

where $V_1$ is the terminal fall velocity of the particle with the portion X removed.

This of course assumes that both particles are falling in the same fluid with the same orientation at constant temperature.

Now taking

$$C_{d1} - C_{do} = cK \left( \frac{V_o^2 - V_1^2}{\left( V_1 V_o \right)^2} \right) = Z \qquad (3.4)$$

where the initial conditions may be taken as a constant, it is now possible to determine how $C_{d1} - C_{do}$ changes with velocity.

$$\frac{\partial Z}{\partial V} = -\frac{cb}{V_1^3}$$

and

$$\frac{\partial^2 Z}{\partial V^2} = \frac{ca}{V_1^4}$$

where a and b are constants.

This indicates the graph of $\frac{Z}{cK}$ versus $V_1$ is similar in form to that shown in Fig. 2.

Since $V_1$ is less than $V_o$; $C_{d1}$ is greater than $C_{do}$; and $Re_o$ is greater than $Re_1$, the general shape of the $C_d$ versus Re relation should be as shown in Fig. 3; where the subscripts $_o$ and $_1$ refer to the original particle and the particle with the portion X removed respectively.

In the inertial region however, previous research has indicated that $C_d$ becomes independent of Re and approaches a constant value as shown by the dashed lines on Fig. 3. This illustrates the fact that the Corey shape factor alone does not describe the particle adequately.

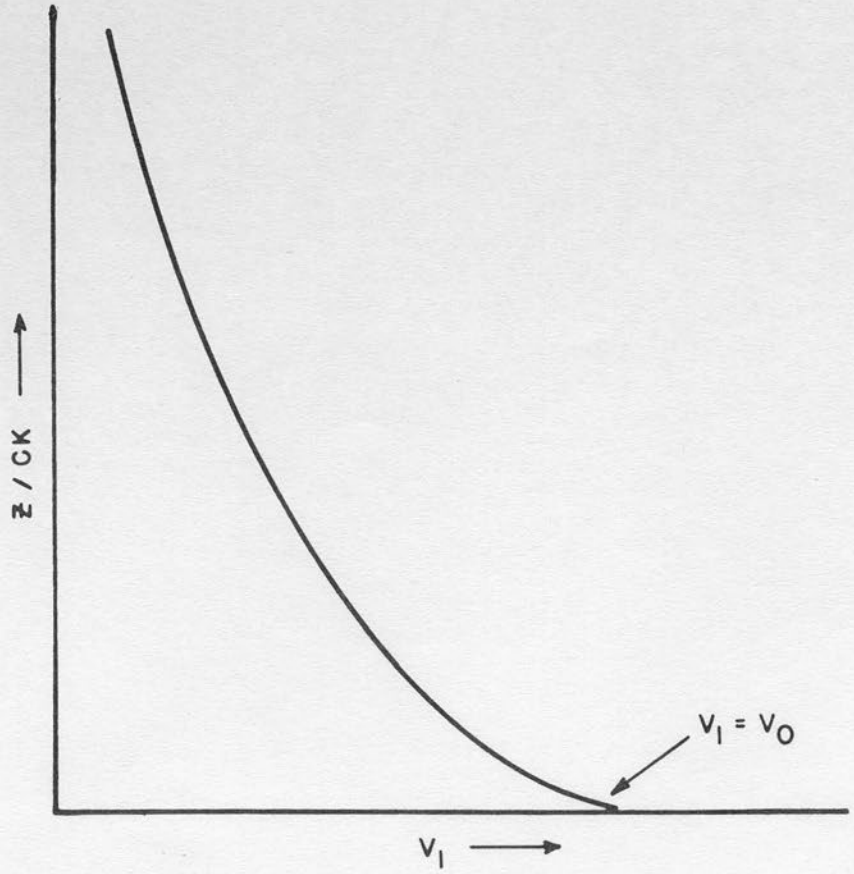


FIG. 2 GENERAL VARIATION OF CHANGE IN THE DRAG FORCE WITH CHANGE IN VELOCITY CAUSED BY MODIFICATION OF PARTICLE SHAPE

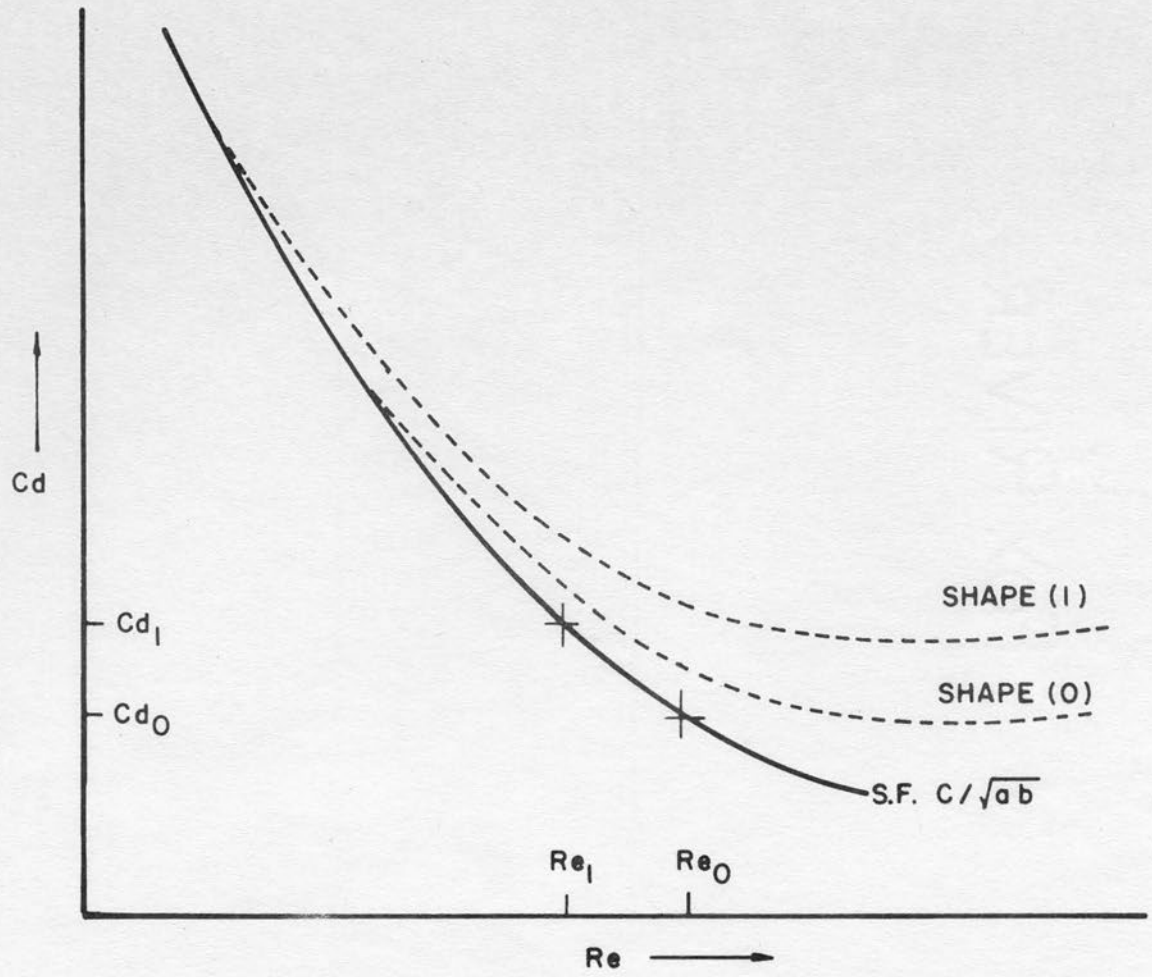


FIG. 3 GENERAL VARIATION OF DRAG COEFFICIENT WITH REYNOLDS NUMBER FOR MODIFICATIONS OF PARTICLE SHAPE

For the previous analysis to be valid in comparison to concepts of pressure drag, the change from particle (o) to particle (1) by removal of the portion X actually shifted from one shape curve vertically to that of another shape curve.

It appears that an expression of particle shape may be influenced by several parameters. The Corey shape factor of a sphere is 1.00 and since shape factor is a good measure of flatness and has already proved to be a fairly good indication of the orientation of the curves for various particles in the $C_d$ versus Re relationship, it seems advantageous to combine it with similar expressions which relate particle roughness, angularity and surface area. The purpose of this study is to determine the effect and necessary modifications relating to surface area.

Since the sphere has been thoroughly investigated and its relationship in the $C_d$ versus Re diagram is quite sound, it seems wise to use it as a base from which to measure other particles. The Corey shape factor, as it has been used, places the sphere (S.F. = 1) at the lower portion of the $C_d$ versus Re diagram. The results of tests on other shapes (Corey shape factor less than 1) show curves situated above the sphere curve with values of shape factor decreasing in the vertical direction. Then with the vertical shift shown in Fig. 3 with the removal of the portion X (S.F. = constant), the correction applied to the Corey shape factor must be such that it would decrease the Corey shape factor in order to account for the effect of surface area change.

A correction which would tend to indicate the distribution of surface area and at the same time maintain a shape parameter equal to 1.00 for spheres would be the ratio of $\frac{d_A}{d_n}$ or $\frac{d_n}{d_A}$.

$d_n$ is the diameter of a sphere having the same volume as that of of the particle (nominal diameter)

$d_A$ is the diameter of a sphere having the same surface area as that of the particle

It must now be shown that either $\frac{d_A}{d_n}$ or $\frac{d_n}{d_A}$ is a function decreasing in absolute value.

With reference to Fig. 1

$$V = \frac{\pi d_n^3}{6} \quad \text{or} \quad d_n = \sqrt[3]{\frac{6V}{\pi}} = c_1\sqrt[3]{V}$$

and

$$S = \pi d_A^2 \quad \text{or} \quad d_A = \sqrt{\frac{S}{\pi}} = c_2\sqrt{S}$$

then

$$\frac{d_{Ao}}{d_{no}} = \frac{c_2\sqrt{S}}{c_1\sqrt[3]{V}} = c_3\frac{\sqrt{S}}{\sqrt[3]{V}}$$

for the original particle where $c_1$, $c_2$, and $c_3$ are constants.

Then for the particle with portion X removed

$$\frac{d_{A1}}{d_{n1}} = \frac{c_3\sqrt{S - 2S'}}{\sqrt[3]{V - cS'}} = c_3 Z_1$$

where

$$Z_1 = \frac{\sqrt{S - 2S'}}{\sqrt[3]{V - cS'}}$$

then

$$\frac{dZ_1}{dS'} = \frac{\frac{c}{3}(S - 2S')^{1/2}(\forall - cS')^{-2/3} - (S - 2S')^{-1/2}(\forall - cS')^{1/3}}{(\forall - cS')^{2/3}}$$

or

$$(\forall - cS')^{2/3}\frac{dZ_1}{dS'} = \frac{c}{3}(S - 2S')^{1/2}(\forall - cS')^{-2/3} - (S - 2S')^{-1/2}(\forall - cS')^{1/3}$$

and

$$\frac{dZ_1}{dS'}(\forall - cS')^{4/3}(S - 2S')^{1/2} = \frac{cS}{3} + \frac{cS'}{3} - \forall$$

which with further refinement yields

$$\frac{dZ_1}{dS'}(\forall - cS')^{4/3}(S - 2S')^{1/2}\frac{3}{c} = S + S' - \frac{3\forall}{c} \qquad (3.5)$$

where the sign of all the terms on the left are positive with the exception of the unknown $\left(\frac{dZ_1}{dS'}\right)$, then if it can be shown that the net sign of $\left(S + S - \frac{3\forall}{c}\right)$ is negative, $\left(\frac{dZ_1}{dS'}\right)$ must be negative and the function is a decreasing one.

For small c and s' and an area and volume approximation of $S = 2ab$, $\forall = abc$, the right side of the equation becomes $(s' - ab)$ where s' is much less than ab or the sign is negative and the function $\frac{d_A}{d_n}$ is a decreasing function. This suggests a new shape parameter

$$(S.F.)\left(\frac{d_A}{d_n}\right) \qquad \text{where} \quad S.F. = \frac{c}{\sqrt{ab}}$$

## E. REYNOLDS NUMBER

It is also necessary to investigate the Reynolds number since it has been customary to use $d_n$ as the characteristic length in the Reynolds number equation. It may be that $d_A$ would be a better characteristic length for particle descriptions.

Reynolds number is defined as the ratio of inertia force to that of the resistance force due to viscosity

or

$$Re = \frac{F_I}{F_v} = \frac{Ma'}{\mu \frac{dv}{dy} A} = \frac{\rho \forall \frac{V^2}{2}}{\mu \frac{V}{L} A} = \frac{\forall V}{\nu A} = \frac{c d_n^3 V}{\nu A} \qquad (3.6)$$

where $A$ is the area on which the viscous shear acts. This area is not necessarily the total area nor is it a constant.

From a simple type of dimensional analysis Reynolds number becomes

$$Re = \frac{\rho V^2 L^2}{\mu VL} = \frac{VL}{\nu} \qquad (3.7)$$

where $L$ is customarily thought of as some representative length for the particle in question and in the $C_d$ versus $Re$ relationships for irregular particle $L$ has been taken as $d_n$.

If one regards a sphere made of putty with a diameter $d_n$ and then molds the putty into various other shapes it is apparent that $d_n$ stays the same for all shapes and is thus not a characteristic length for the particles. However, if one regards $d_A$ as the characteristic length it is also apparent that this would in effect distinguish the different forms

with the same $d_n$ value. Thus it would appear better to use $Re = \frac{Vd_A}{\nu}$ for the Reynolds number.

## F. DRAG EQUATION

In making use of the drag equation as indicated by equation 3.1 the area term has been customarily taken as $\frac{\pi d_n^2}{4}$. For irregular shapes this does not seem to be indicative of area. Taking the drag equation in the form

$$C_d = \frac{\left(\frac{\pi}{6}\right) d_n^3 \left(\rho_s - \rho_f\right) g}{A \rho_f \frac{V^2}{2}}$$

and with area equal to $\frac{\pi d_n^2}{4}$, the equation is modified to

$$C_d = \frac{4}{3} \frac{d_n \left(\rho_s - \rho_f\right) g}{\rho_v V^2} \qquad (3.8)$$

for irregular shapes as well as for spheres.

However, in the initial equation it is seen that A is intended to represent the cross sectional area of the particle normal to the direction of fall. From the analysis of the ball of putty in the section on Reynolds number, it is seen that here again $d_n$ is not necessarily a function of such an area for the irregular shape. Again making use of $d_A$ instead of $d_n$, the drag equation becomes:

$$C_d = \frac{4}{3} \left(\frac{d_n}{d_A}\right)^2 \frac{d_n \left(\rho_s - \rho_f\right) g}{\rho_f V^2} \qquad (3.9)$$

However, it must be recognized that

$\frac{\pi d_n^2}{4}$ and $\frac{\pi d_A^2}{4}$ are not necessarily representative

of the true area term in the drag equation. The term $d_A$ may only appear to be a better indication than $d_n$. Furthermore, the correction $\left(\frac{d_n}{d_A}\right)^2$ from the analysis above may be too extreme and the exponent may have to be determined experimentally.

# CHAPTER IV

## EXPERIMENTAL EQUIPMENT AND PROCEDURE

The terminal fall velocities of the gravel particles were determined by a photographic technique. The particles were dropped in the fall column in a dark room. A stroboscope of known frequency was placed at the top of the column and the flashing light used as the light source to form the images with a polaroid camera located at a fixed distance from the column.

A graduated scale was suspended in the fall column at various points in order to determine the scale factor to be applied to the photographs and to apply a correction to particles not falling in the exact center of the column. From the photographs of the scale suspended in the fluid, plastic overlays were constructed that could be placed over the photographs of the particles to obtain the fall velocities.

The fall velocity could then be computed from the equation

$$V = C\frac{D}{N}\frac{f}{60} \tag{4.1}$$

where

C is the correction applied for a particle not falling along the center line of the fall column,

D is the distance between two images taken from the plastic overlay,

N is the number of image spaces between the two selected for measurement,

f is the frequency of the stroboscope in rpm.

It was necessary to devise a different means of obtaining the terminal fall velocity of the larger particles. These particles were too large to be dropped in the fall column because of the limited length and diameter of the column. These larger particles were eventually dropped in a reservoir from the side of a boat. A special technique was devised to measure the fall velocity and is described in section 6 of this chapter.

A. Components of the Equipment

1. Fall Column - The fall column consisted of a vertical plexiglass tube 1/4 inch thick, 16 inches inside diameter, and ten feet high. The bottom of the column was sealed with a 1/2 inch thick inclined plastic plate such that the particle as it struck the bottom would slide down the incline. A plastic tube outlet equipped with plastic hose and pinch clamp was located at the bottom of the incline. A plastic receiver cup was inserted at the outlet in order to collect the particles. A circular cotton fabric screen was suspended on a brass ring about 3 inches from the bottom of the plate. This screen was used to catch the particle before striking the bottom. With slight alternate pulling and releasing of the cords which suspended the ring, the particle was caused to slide down the fabric to an opening located near the tubular outlet of the fall column. Directly opposite the plastic tube outlet was a second opening into the fall column. This outlet was sealed with a rubber stopper with a long

brass rod extending through the center of the stopper and into the fall column. This rod could then be used to position the particles better for extraction from the fall column.

A background of black fabric was provided in the lower section of the fall column for contrast.

Four thermometers were provided at various points in the fall column to determine the temperature differential in the column.

At the left of the column a mirror was provided in order to show a view 90 degrees to that of the line of the camera. This view as it appeared in the photographs was used as a means of correcting fall velocity for particle position.

2. Partial Release - An attempt was made to use a mechanical release consisting of a steel frame on which was mounted a steel jaw. The jaw could be opened by pulling on a cord which led back to the position of the camera. However, this proved to be unsatisfactory as a dropping mechanism for irregular particles. Better results were obtained by simply holding the particle with its largest cross-section normal to direction of fall between the thumb and forefinger about one inch under the surface and making the drop from this position. Other drop positions and orientations were tried but in all cases the particle would orient with its major cross-section normal to the direction of fall in a relatively short distance.

3. Stroboscope - The specifications for the stroboscope used in this investigation are as follows:

Flashing rate - 110 to 25,000 flashes per minute in three ranges: 110-690, 670-4170, and 4,000-25,000.

Accuracy - 1 percent of dial reading after calibration in the middle range.

Calibration - could be calibrated against power line frequency by panel screwdriver adjustment.

Flash duration - approximately 1, 3, and 6 microseconds for high, medium, and low speed ranges, respectively (measured at 10 percent of maximum intensity).

Peak light intensity - 0.21, 1.2, and 4.2 million candlepower minimum on high, medium, and low speed ranges respectively. For single flash, 7 million candlepower.

Reflector angle - 10 degrees at half intensity points.

4. Scale - A calibration scale was made by marking a white painted steel tape at five centimeter intervals. The scale was then weighted at the lower end and suspended in the fall column for each of the several fluids used during the test.

5. Camera and film - A Polaroid Land Camera, Model 95B, was used for this investigation.

The film was Polaroid type 47 having a speed of ASA 3200. The prints obtained were 3-1/2 by 4-1/2 inches.

A sketch arrangement of this equipment is shown in figure 4 and a photograph of the equipment is shown in figure 5.

6. Velocity Measurement of Large Particles - The rear wheel and hub from an English racing bike were mounted in a steel bracket which in turn could be fastened to the back of a boat much like an outboard motor. The wheel was fitted with a hand operated brake as well as a mechanical brake system which could be adjusted and set to any desired degree of bearing resistance for the wheel. A light spring steel wire was then fastened on the periphery of the wheel in such a way as to protrude out radially from the rim. A 1/16 inch diameter, 150 lb. test nylon cord was then wrapped around the rim and the particle to be dropped fastened to the loose end of the cord. As the particle fell through the water the wheel would turn and as it turned the spring steel wire would strike an insulated metal contact with each revolution. The bracket holding the wheel and the insulated contact were then connected in series with a 45 volt D. C. battery and a 28 volt D. C. counter.

In this manner each revolution of the wheel was recorded by the counter. A stop watch was then used to time a series of revolutions and the fall velocity computed from

$$V = \frac{N'C'}{T}$$

where

V is the velocity in cm/sec,

N' is the number of revolutions,

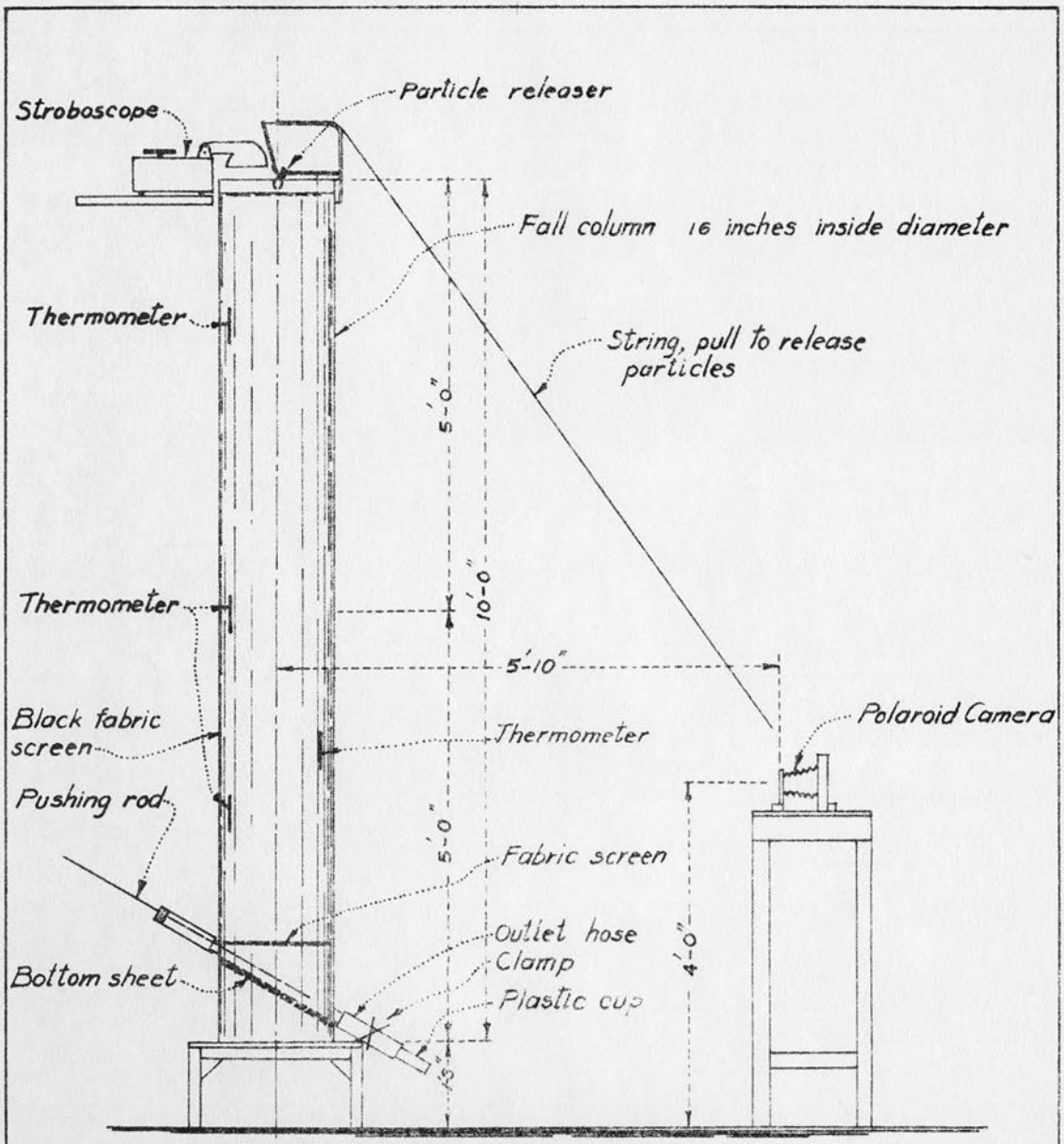


FIG. 4 ARRANGMENT OF EQUIPMENT USED IN THE FALL VELOCITY STUDY OF IRREGULAR SHAPES

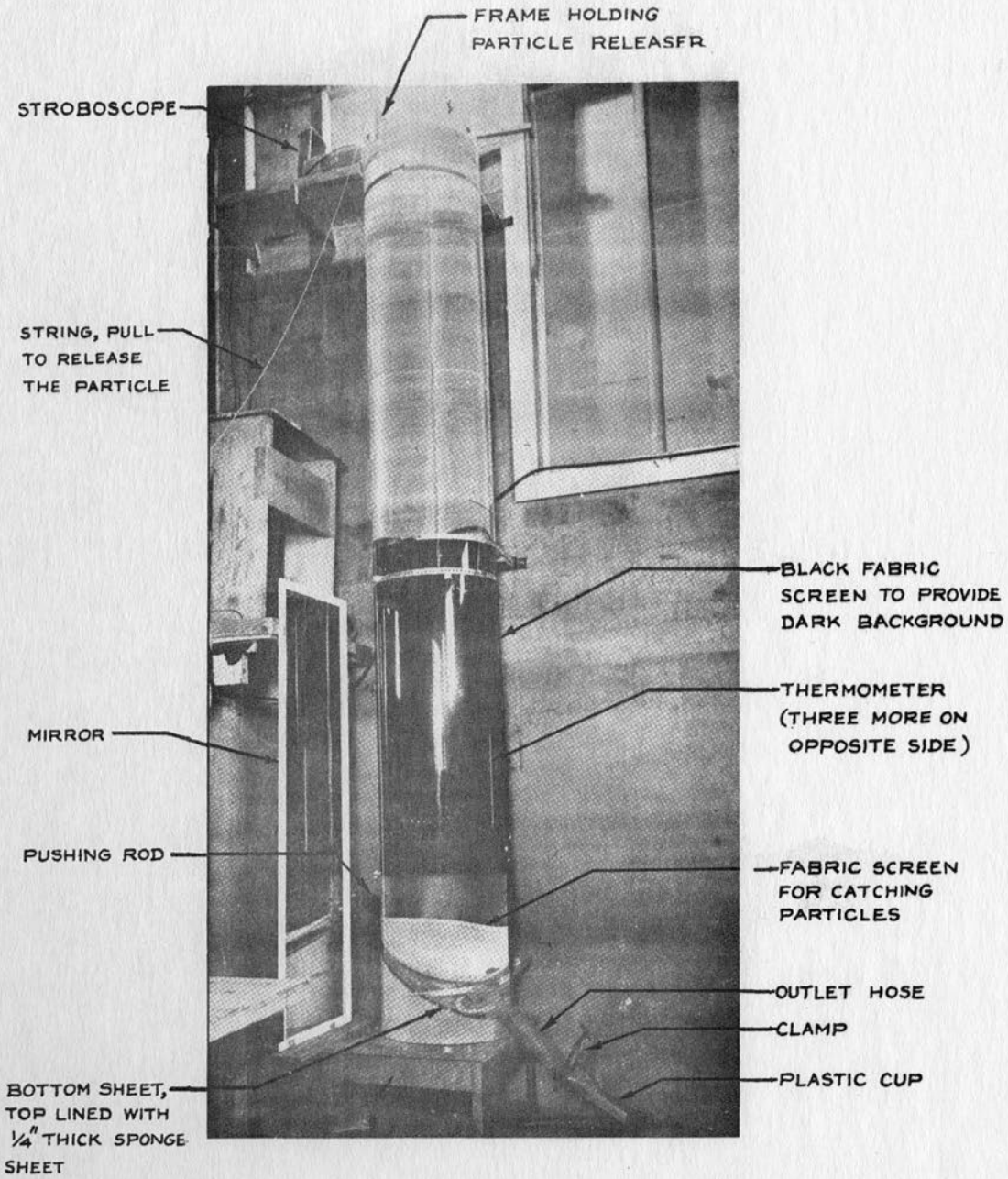


FIG. 5 FALL COLUMN

$C'$ is the circumference of the wheel (cm),

T is the time in sec.

The wheel was allowed to go through two revolutions before beginning to count to insure that the particle had fallen a sufficient distance to reach terminal fall velocity.

B. Particle Surface Area Determination

At this point a method had to be devised for measuring the surface area of the irregular shapes. Two methods were tried and a description of the procedure used and results obtained follows.

1. Wax Method - In the wax method regular household wax was melted in a glass beaker which was held at 75 degrees centigrade in a constant temperature water bath. The gravel specimens were placed in a temperature-controlled oven. The temperature setting of the oven was also maintained at 75 degrees centigrade and checked periodically with a thermometer. Each piece of gravel had been previously spray painted with "Tempo" brand, No. 6004 Callion Gold lacquer to prevent the absorption of additional moisture and also to give the necessary light reflectivity for photographing during the fall velocity tests.

After the particles had been in the oven a sufficient length of time to reach a temperature of 75 degrees centigrade and all of the excess moisture had been driven off, they were removed and each one was weighed separately and the weights were recorded. The balance used was a Voland and Son's Chainomatic analytic type with capability to

0.0001 gram. After weighing, the particles were placed in the oven at 75 degrees centigrade.

After allowing the particles to reach a temperature of 75 degrees centigrade, an individual particle was removed from the oven with a surgical tweezer and immediately suspended in the melted wax for a period of ten seconds, after which it was removed and allowed to drip freely in the room air at 18 degrees centigrade. After all dripping had stopped (approximately 10 seconds) the particle was immersed in water at room temperature (18 degrees centigrade) and the wax allowed to set. The particle was then weighed again (with the wax coating) and the weight recorded. This process was repeated for all the particles, taking care to observe the same minimum contact of particle and tweezer. The wax was removed from the particles by immersion in hot water after which the particles were again placed in the 75 degree oven and allowed to come back to temperature equilibrium. This process was repeated ten times and an average weight of wax was computed for each particle for the ten trials. Duplication of results was reasonably consistent (see table 1).

At this point a special particle was selected (of the same material as the gravels) which was of such a shape that a relatively small amount of grinding transformed the particle into one which had a shape that allowed physical measurements of its size to be made and calculation of its surface area. (A round particle and a flat one were selected in order

to determine if different amounts of wax would adhere to the particle per unit of surface area. The two extremes in shape showed essentially the same weight of wax per unit of area.)

After determining the average weight of wax (ten trials) for the particles of known surface area, a factor of grams of wax per unit surface area was calculated and applied to the particles of unknown surface area to determine the surface area of the irregular shapes.

2. Fluorometer Method - The possibility of using the fluorometer to determine surface area of gravel-sized particles was suggested by Daryl B. Simons.

In this method 150 milliliters of distilled water was placed in a beaker and to this was added 0.40 grams of "labtone" glass cleaner and 0.10 grams of Rhodamine B red dye. The glass cleaner was used to modify surface energy effects. This solution, as well as the gravel particles, was allowed to reach room temperature (22 degrees centigrade).

Each particle was thoroughly washed using the glass cleaner to create the same surface energy effects as the solution. At this point each particle was separately immersed in the dye solution (using the surgical tweezers) for a period of 15 seconds, after which it was removed and allowed to drip freely in air (22 degrees centigrade for approximately 10 seconds). The particle was then dropped into a beaker which contained 300 milliliters of pure distilled water. The beaker

(now containing the particle) was agitated thoroughly so that the dye solution that adhered to the particle would go into solution with the 300 milliliters of water. Some of this solution was then decanted off into a small test tube which, in turn, was placed in the fluorometer (the fluorometer was a G. K. Turner, Model no. 111, which had been zeroed using distilled water).

The reading of the instrument was observed and recorded, the particle washed again, and the process repeated for each particle. An average of the readings for ten trials was computed for each particle. Again there was reasonably good consistency between the readings for an individual particle. A factor then was obtained from the average reading of the particles of known surface and expressed as gage reading per unit surface area. There again appeared to be little difference in unit adhesion between the round and the flat calibrating particles. The unit adhesion factor was applied to the particles of unknown surface area which in turn yielded the surface area of the irregular particles.

3. Conclusions and Comparison of Results - The surface areas obtained from the fluorometer method required less accurate controls, was easier to operate, and was less time consuming than the wax method.

The temperature, controls, and amounts of materials used in either method have been given only for means of clarity in explanation. Since anyone making such tests must calibrate using properties affiliated with some standard particle, the properties and controls expressed here

in these tests could be altered to fit the new situation as long as they remained consistent.

Table I shows the measured quantities using both methods as well as the standard deviation of the ten trials. The standard deviation was computed from

$$Sx = \sqrt{\frac{\sum x^2 - \frac{(\sum x)^2}{n}}{n - 1}} \qquad (4.2)$$

C. Particle Properties

Ten particles were carefully selected to cover a range in shapes from spherical to flat. A photograph of the ten particles used, is shown in figure 6. The symbol shown on each card is used to plot the results of tests on graphs. Particle 1 is a glass marble and was chosen in order to provide a check on the $C_d$ versus Re relation for spheres for each series of drops or viscosity of fluid. On the flat end of the scale, particle 2 was selected on the basis of its round flat characteristics and particle 3 for its flat rectangular character.

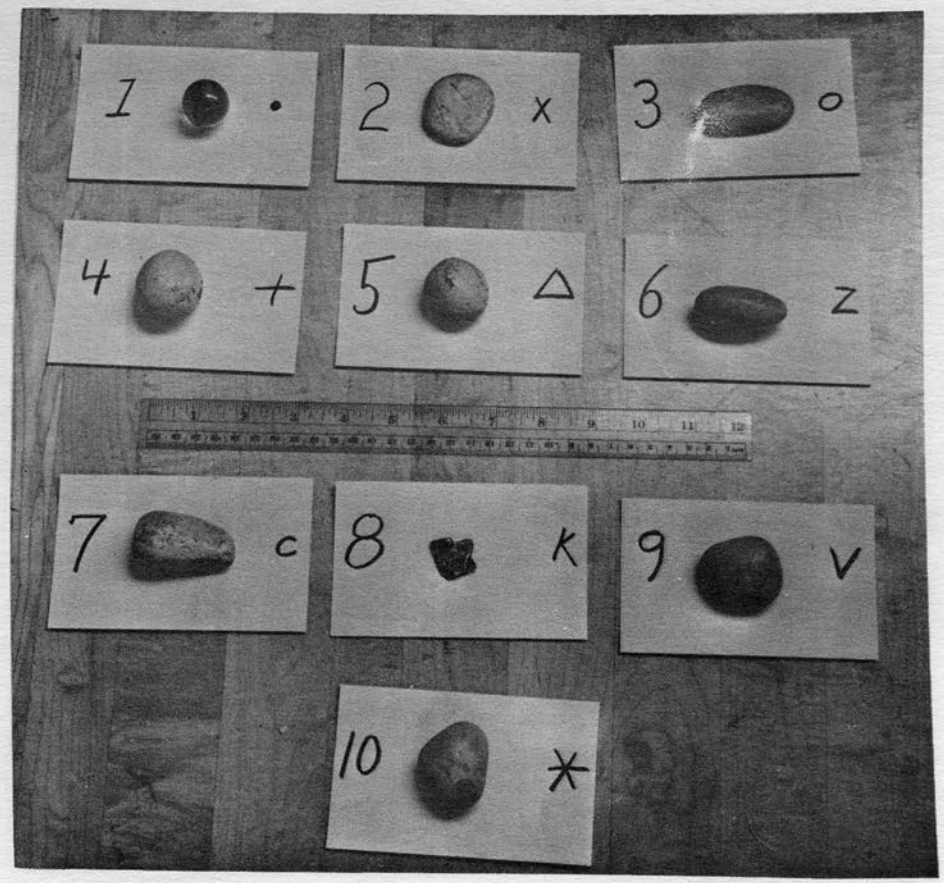


GRAVEL-SIZED PARTICLES

FIG. 6. PHOTOGRAPH OF THE IRREGULAR GRAVEL-SIZED PARTICLES SHOWING THE LETTERING AND NUMBERING SYSTEMS USED TO DESIGNATE EACH PARTICLE

TABLE I

COMPARISON OF SURFACE AREAS FOR IRREGULAR PARTICLES BY THE WAX AND FLUOROMETER METHODS

| Part number | $d_n$ cm | S.F. | Wax method | | Fluorometer method | |
|---|---|---|---|---|---|---|
| | | | Area $cm^2$ | Sx $cm^2$ | Area $cm^2$ | Sx $cm^2$ |
| 2 | 2.44 | 0.22 | 40.8 | 0.95 | 37.0 | 3.9 |
| 3 | 2.62 | 0.31 | 39.9 | 2.2 | 37.2 | 4.5 |
| 4 | 3.28 | 0.74 | 57.8 | 3.7 | 55.7 | 2.9 |
| 5 | 2.99 | 0.75 | 46.8 | 3.3 | 47.7 | 2.3 |
| 6 | 3.06 | 0.67 | 41.4 | 3.4 | 44.8 | 2.9 |
| 7 | 3.31 | 0.56 | 56.0 | 5.0 | 55.2 | 2.9 |
| 9 | 3.24 | 0.64 | 50.7 | 4.8 | 47.6 | 5.2 |
| 10 | 3.28 | 0.73 | 49.9 | 3.2 | 53.4 | 4.2 |

Particles 4 and 5 possessed nearly spherical character but of different densities and size. Numbers 6 and 7 were of egg-shaped appearance with different size and specific weight. Particle 8 was a relatively flat piece of mica. However, this particle was not suitable for study since it had a tendency to flake off and to take on considerable amounts of moisture between the mica layers. Particles 9 and 10 were of completely irregular character but at the same time similar in nature to each other. All particles were oven dried and then spray painted a yellow color in order to give a good light reflectively and to avoid absorption of moisture during testing.

The density of the particles was found by weighing in air and then in distilled water from the relation

$$\rho_p = \frac{Wa\ \rho w}{Wa - S}$$

where

Wa is the dry weight in air,

$\rho w$ is the density of water,

S is the scale reading of submerged weight

$\rho_p$ is the density of the particle,

Particle volume is then

$$\forall = \frac{Wa - S}{\rho w}$$

and

$$d_n = \sqrt[3]{\frac{6}{\pi}\left(\frac{Wa - S}{\rho w}\right)} = \sqrt[3]{\frac{6}{\pi}\frac{Wa}{\rho_p}} \qquad (4.4)$$

where $d_n$ is the nominal diameter (see table number II).

TABLE II

PROPERTIES OF GRAVEL-SIZED PARTICLES

USED IN FALL VELOCITY TESTS

| Particle number | Symbol | $d_n$ cm | $d_A$ cm | gm/cm² | S.F. | S.F. $\left(\frac{d_A}{d_n}\right)$ |
|---|---|---|---|---|---|---|
| 1 | θ | 2.49 | 2.49 | 2.47 | 1.00 | 1.00 |
| 2 | X | 2.44 | 3.51 | 2.93 | 0.22 | 0.32 |
| 3 | 0 | 2.62 | 3.50 | 2.91 | 0.31 | 0.41 |
| 4 | + | 3.28 | 4.25 | 2.57 | 0.74 | 0.96 |
| 5 | Δ | 2.99 | 3.88 | 2.59 | 0.75 | 0.97 |
| 6 | Z | 3.06 | 3.70 | 2.96 | 0.67 | 0.81 |
| 7 | c | 3.31 | 4.20 | 2.98 | 0.56 | 0.71 |
| 8 | K | 1.36 | ---- | 2.70 | 0.22 | ---- |
| 9 | V | 3.24 | 3.96 | 2.59 | 0.64 | 0.78 |
| 10 | * | 3.28 | 4.06 | 2.63 | 0.73 | 0.90 |

As a check on the results obtained from the irregular shapes several particles were machined from aluminum in order that the shapes used would have some mathematical expression for volume and surface areas. Disks, spheroids and rods were selected. One of the disks was 1-1/2 inches in diameter and 5/32 inch thick. The other was 1 inch in diameter and 1/8 inch thick or a scale factor of 0.5. The larger of the two spheroids had a major axis of 1-1/2 inches, and minor, of 3/4 inch while the smaller had a major axis of 1 inch and a minor of 1/2 inch or a scale factor of 2/3. The scale factors referred to,

represent the multiple by which representative lengths of one size were modified in order to obtain another size but of the same shape. These particles were dropped in water (11 degrees centigrade) and the fall velocity results as well as particle properties are given in table III.

The large particles used consisted of a regulation size concrete test cylinder and two steel cylinders of different sizes. The properties of these particles are given in table IV.

D. Fluids

In order to cover a range of Reynolds Numbers for each individual particle, various mixtures of glycerene and water were used to obtain different viscosities for the surrounding medium. In this manner, a wide range of viscosities could be covered and a clear solution could be maintained for taking photographs.

The viscosities of the fluids were obtained using a Stormer viscosimeter and curves showing viscosity as a function of temperature are given in figure 7. The densities of the solutions are given in figure 8.

The water and glycerene were mixed using a centrifugal pump connected to the outlet of the fall column and pumping back into the top of the fall column. The pump was run for approximately three hours to insure thorough mixing. After the pump was shut down the fluid was left to stand in the fall column for about three days in order for all air bubbles to escape and turbulence to dissipate. Only water was used for the large particles and the machined shapes.

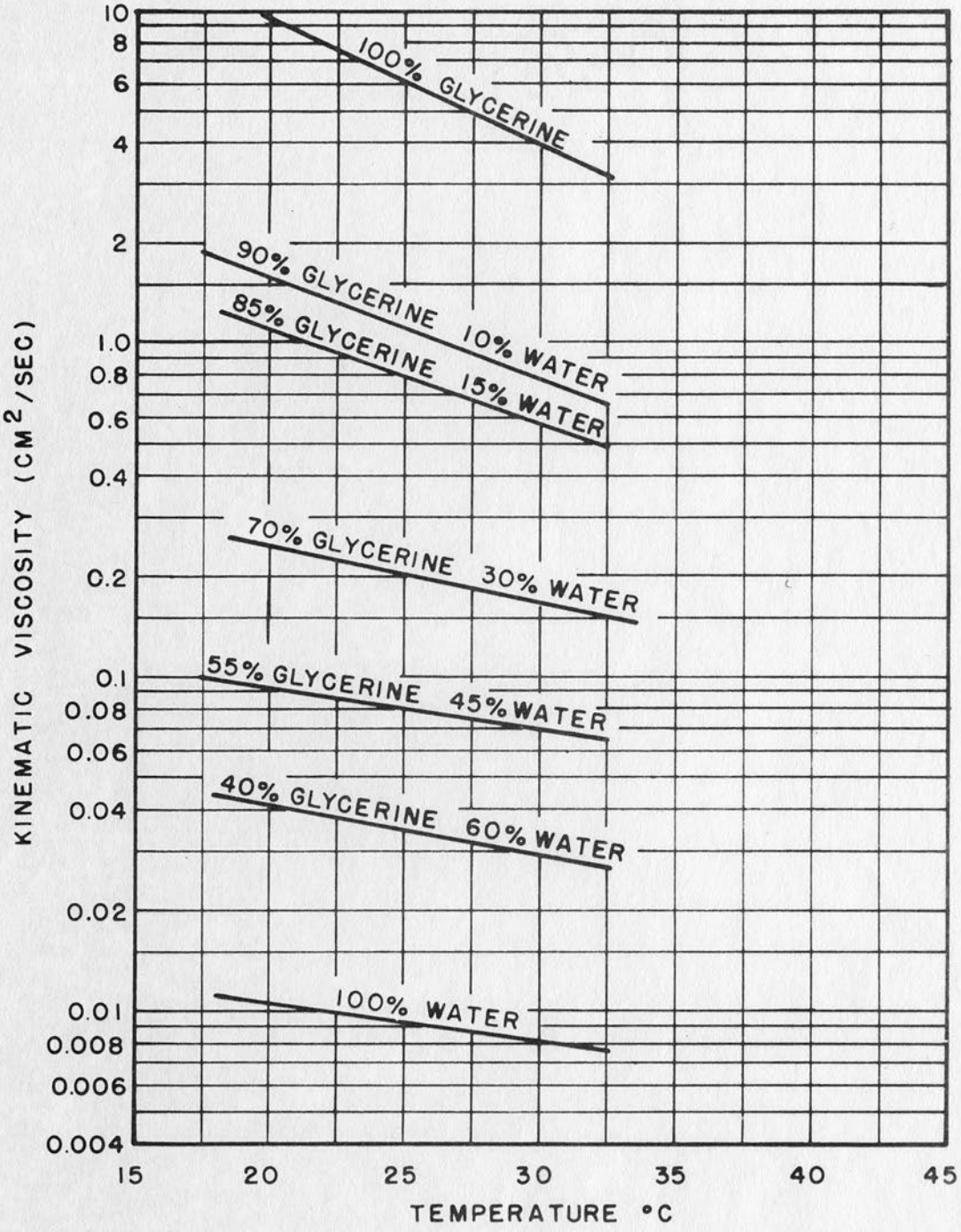


FIG. 7 VARIATION OF KINEMATIC VISCOSITY WITH TEMPERATURE FOR THE TEST SOLUTIONS

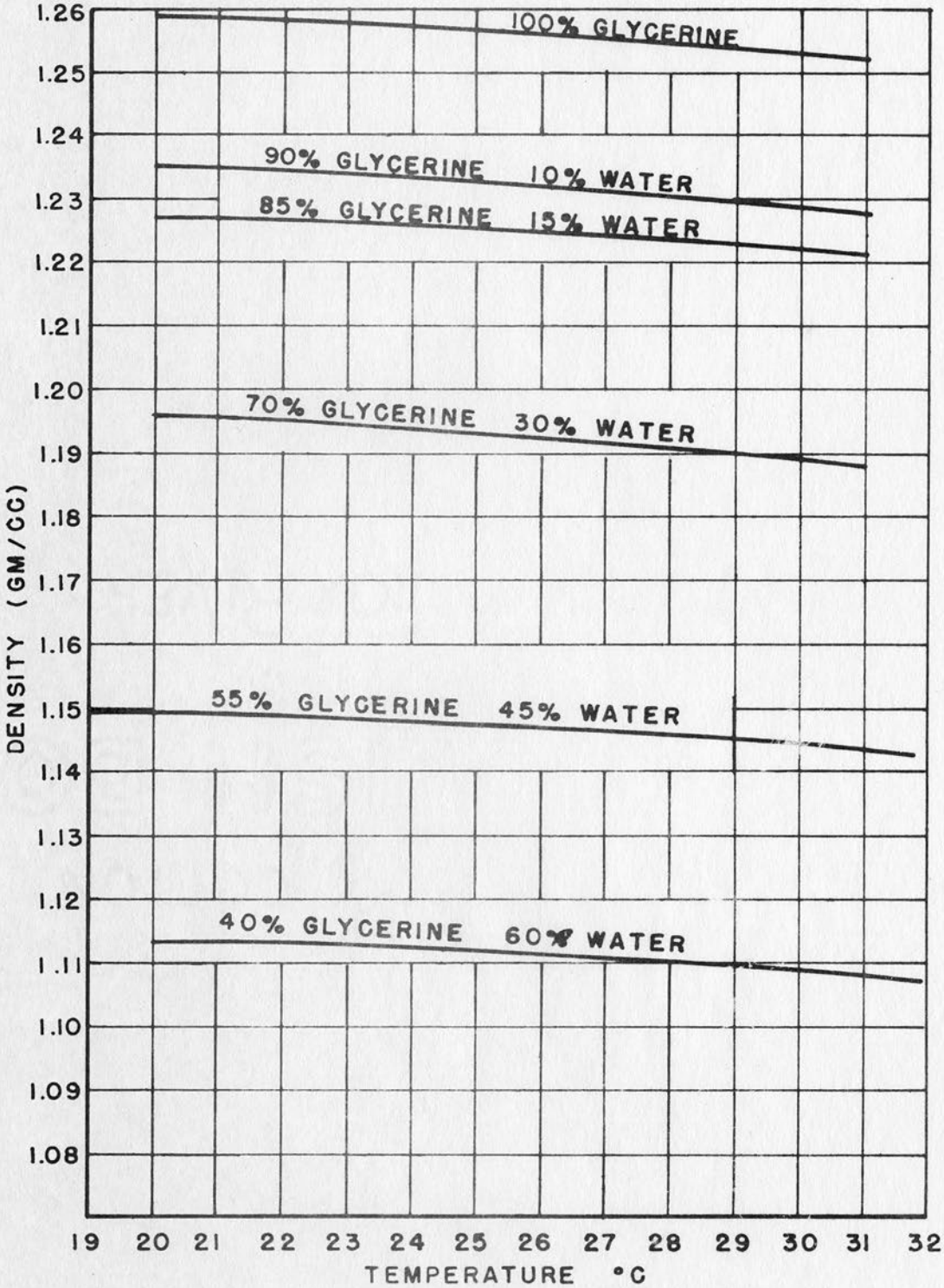


FIG. 8 VARIATION OF DENSITY WITH TEMPERATURE FOR THE TEST SOLUTIONS

TABLE III

FALL VELOCITIES AND PROPERTIES

OF MACHINED PARTICLES

| Particle | Velo. cm/sec. | $\rho_p$ | $d_n$ cm | $d_A$ cm | S.F. | S.F. $\frac{d_A}{d_n}$ | $C_d$ | Re |
|---|---|---|---|---|---|---|---|---|
| 11 | 87.5 | 2.79 | 2.40 | 2.48 | 0.707 | 0.73 | 0.734 | 16,750 |
| 12 | 76.6 | 2.79 | 1.60 | 1.66 | 0.707 | 0.73 | 0.614 | 9,820 |
| 13 | 48.3 | 2.79 | 1.15 | 1.35 | 0.50 | 0.585 | 0.99 | 5,040 |
| 14 | 33.3 | 2.79 | 0.576 | 0.673 | 0.50 | 0.585 | 1.04 | 1,730 |
| 15 | 30.0 | 2.79 | 1.82 | 2.52 | 0.125 | 0.173 | 3.42 | 5,850 |
| 16 | 28.0 | 2.79 | 1.46 | 2.00 | 0.125 | 0.173 | 3.19 | 4,330 |

Key:

11 is the large spheroid.
12 is the small spheroid.
13 is the large rod.
14 is the small rod.
15 is the large disk.
16 is the small disk.

TABLE IV

FALL VELOCITIES AND PROPERTIES

OF STEEL AND CONCRETE CYLINDERS

| Particle | Velo. cm/sec | $\rho_p$ gm/cc | $d_n$ cm | $d_A$ cm | S.F. | S.F. $\frac{d_A}{d_n}$ | $C_d$ | Re |
|---|---|---|---|---|---|---|---|---|
| 17 | 220 | 2.39 | 22.0 | 24.1 | 0.707 | 0.775 | .765 | 483,000 |
| 18 | 204 | 8.19 | 7.77 | 9.62 | 0.389 | 0.481 | 1.47 | 179,000 |
| 19 | 379 | 8.00 | 9.07 | 9.76 | 0.817 | 0.879 | .577 | 307,000 |

Key:

17 is the concrete test cylinder (approximately 6" dia. by 12" long)
18 is a steel cylinder (approximately 1-3/8 dia. by 9-1/2" long)
19 is a steel cylinder (approximately 2-3/4 dia. by 4-1/4" long.)

E. Procedure

The physical size range covered by the particles necessitated two different procedures for the determination of the terminal fall velocities of the particles.

1. Gravel-sized Particles - After the desired fluid had been mixed and allowed to stand a sufficient time the particles were prepared for dropping. Just prior to dropping all particles were immersed in a beaker containing some of the drop fluid. The next step was to adjust the flashing of the stroboscope such that two consecutive images on a photograph were about 1 centimeter apart on the photograph. This usually required a trial drop at a given setting and then an adjustment in order to obtain the desired setting. The camera shutter control was set at "B" with lens opening at f8.8 and triggered by a cable release thus allowing the shutter to be held in an open position by the operator. With the camera set and the stroboscope set at a suitable flashing rate, all lights were turned off, the stroboscope turned on and the particle released. As the particle reached the lower half of the fall column the lens shutter was opened by means of the cable trigger and held open until the particle reached the bottom. Then the lights were again turned on, the picture removed and the stroboscope frequency recorded on the photograph. Figures 9, 10, 11 show pictures of the type used for computation of fall velocity.

2. Large Scale Particles. - The large particles were suspended over the side of the boat by simply holding the bicycle wheel to keep it

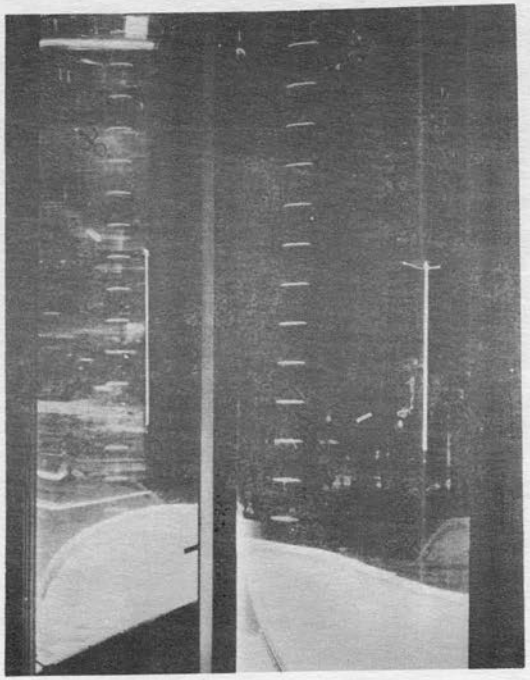

(A) PARTICLE NO. 2

100% GLYC.
200 RPM
23.2° C

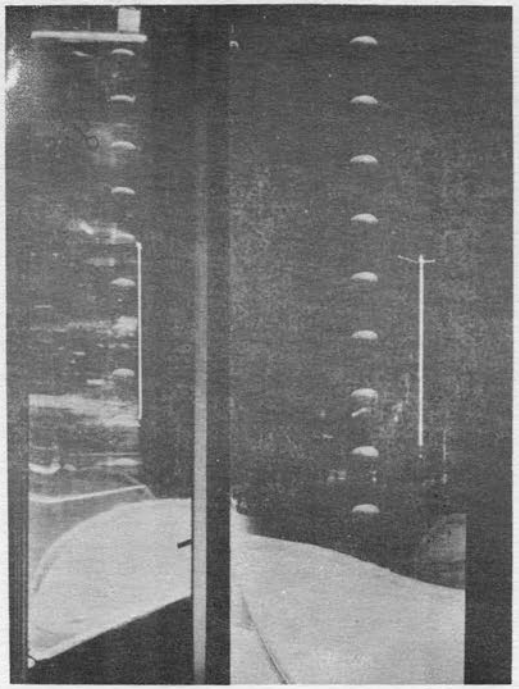

(B) PARTICLE NO. 5

100% GLYC.
200 RPM
23.2° C

FIG. 9. SAMPLE PHOTOGRAPHS OF GRAVEL-SIZED PARTICLES FALLING IN FLUIDS AT VARYING VISCOSITIES

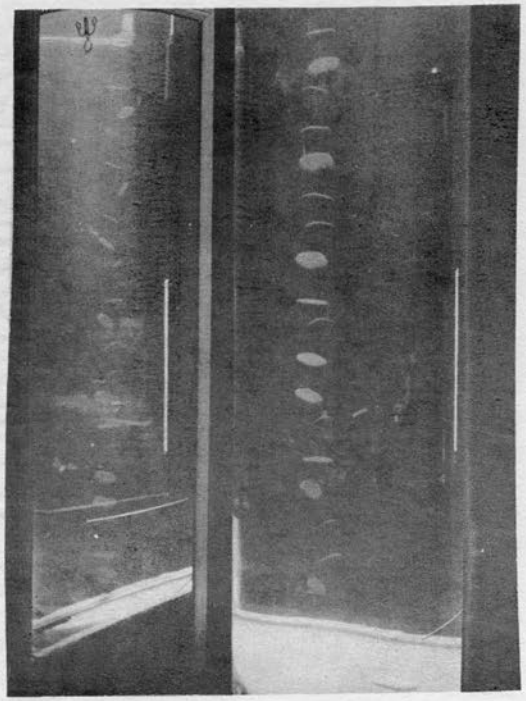

(E) PARTICLE NO. 2

55% GLYC.
500 RPM
19.0° C

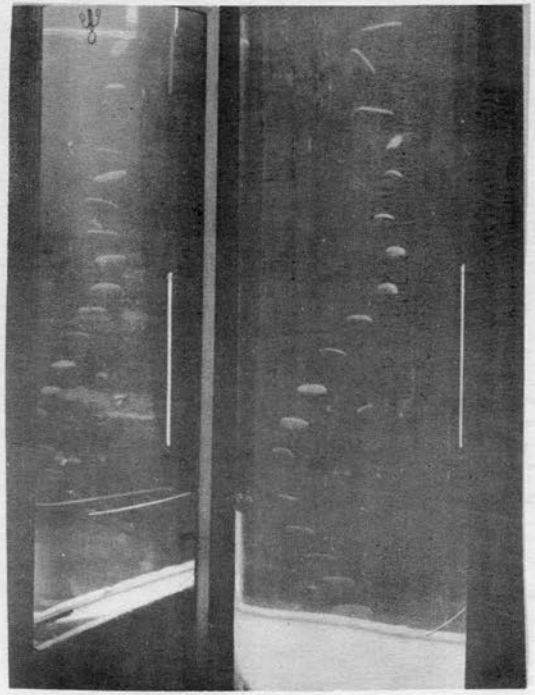

(F) PARTICLE NO. 3

55% GLYC.
500 RPM
19.0° C

FIG. 10. SAMPLE PHOTOGRAPHS OF GRAVEL-SIZED PARTICLES FALLING IN FLUIDS AT VARYING VISCOSITIES

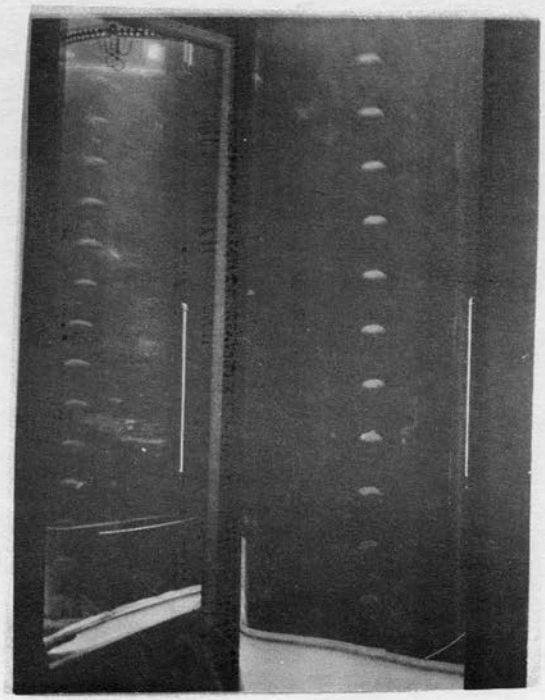

(C) PARTICLE NO. 9

40% GLYC.
600 RPM
20.0° C

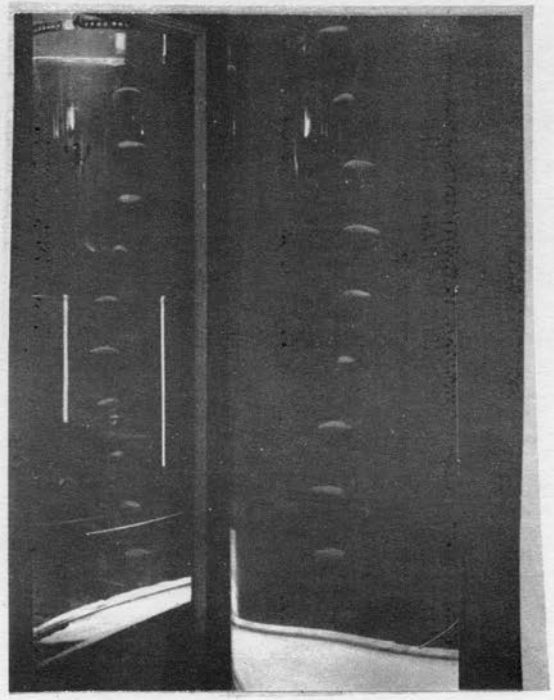

(D) PARTICLE NO. 6

55% GLYC.
500 RPM
13.5° C

FIG. 11. SAMPLE PHOTOGRAPHS OF GRAVEL-SIZED PARTICLES FALLING IN FLUIDS AT VARYING VISCOSITIES

from turning. The particle was then lowered until the spring steel wire had just passed the metal contact point. The wheel was then released and allowed to pass through two revolutions by observing the counter. At the instant the counter recorded the second revolution the stop watch was started and allowed to run until 4 more revolutions had been made at which time the stop watch interval was recorded. With the diameter of the wheel used this involved a fall distance of 692 cm or approximately 22.5 ft. The fall distance divided by the recorded time resulted in the fall velocity. Ten drops were made for each particle and an average time for the ten drops was used to calculate the velocity.

# CHAPTER V

## PRESENTATION AND DISCUSSION OF RESULTS

The results of the study are presented in this section and a description of various particle motions and an analysis of the results of the surface area-shape parameter study are emphasized. Sample photographs of several particles falling at various Reynolds numbers are also presented.

### A. Particle Motion

Figures 9 and 10 show particle number 2 falling at Reynolds numbers of 10 and 1590 respectively. At Reynolds number 10 this round flat particle appears to fall with a quite stable orientation in contrast to the alternate tipping-sliding motion of Fig. 10 at Reynolds number 1590. Intermediate photographs (not shown) indicate this tipping-sliding motion is first observed at a Reynolds number of about 100. Reynolds number at which this motion begins cannot be determined because of the manner of data collection. Other photographs of the same particle indicate a fully developed motion of the type indicated at a Reynolds number of between 700 and 1000. The shape parameter of this particle S. F. $\left(\frac{d_A}{d_n}\right)$ is 0.32 and if one refers to Fig. 14 it is interesting to note that the horizontal portion of the curve relating to this particle begins at a Reynolds number in this same range. The observed rotation of this particle was very slight.

Particle number 3, Fig. 10 is of a flat rectangular nature and has a shape parameter of 0.41. This particle exhibits the

alternate tipping motion between Reynolds number of 123 and 210 (slightly greater than particle number 2) and fully developed tipping and sliding motion between Reynolds numbers of 1000 and 2000. With reference to Fig. 14 the inertial region is again apparently established in this range. Particle rotation was very slight but greater than for particle number 2. An analysis of the more rounded particles (5, 6, and 9) with S. F. $\left(\frac{d_A}{d_n}\right)$ approaching 1.00 indicates this same pattern of development with the tipping-sliding motion becoming less and less pronounced as the shape parameter approached 1.00. Intermediate shapes illustrate the same tendencies considering their observed motion.

One can summarize by saying that in general, increase of S. F. $\left(\frac{d_A}{d_n}\right)$ indicates a decrease in the tipping-sliding motion and an increase in particle rotation.

The period and amplitude of the alternate tipping-sliding motion may be qualitatively explained by referring to the discussion in Chapter III on particle motion. As particle size and surface area are increased for the same general shape (say a disk of increasing diameter) the component of weight and shear forces will increase in magnitude but not necessarily at the same rate. Thus, particle inclination will be altered until the weight component directed along the inclined axis of the particle overbalances the shear. At the same time the separation zone has increased and the degree of influence of the vortex formation has affected the pressure distribution as well as the resulting eccentricity. The

combination of these will in turn have direct influence on the net thrust and net torque exerted on the particle.

B. General Relationships

Three Figs. (12, 13, and 14) are given to illustrate the effects of the proposed corrections outlined in Chapter III. A summary of the pertinent data is given in the Appendix A in Tables VI through XII.

Figure 12 is a reproduction of Fig. 1, page 20 from reference 11. This shows a compilation of results plotting $C_d = \frac{4}{3} \frac{d_n (\rho_p - \rho_f)\, 981}{\rho_f V^2}$ versus $Re = \frac{V d_n}{\nu}$ with the Corey shape factor (S. F.) as the third variable. The lines of constant shape factor are average lines determined from data with considerable scatter. This plot is shown for comparison with the new plots resulting from this study. The original data collected by others and used to construct the lines of constant shape factor have been omitted while the results of this investigation have been superimposed in order to show the need for further refinement. The collection of this data was accomplished by dropping different particles through the same fluid. The size of the particle was then the criterion for changing the Reynolds number. If one refers to the particle properties listed in Table II, it is apparent that particles do not behave as the lines of constant shape factor would predict. For example, particle X has a Corey shape factor of 0.22, yet it appears to follow the shape factor line of 0.30. The plot of the data appears to indicate a dip through a certain range of Reynolds number, depending on the shape factor. This dip is not apparent in the

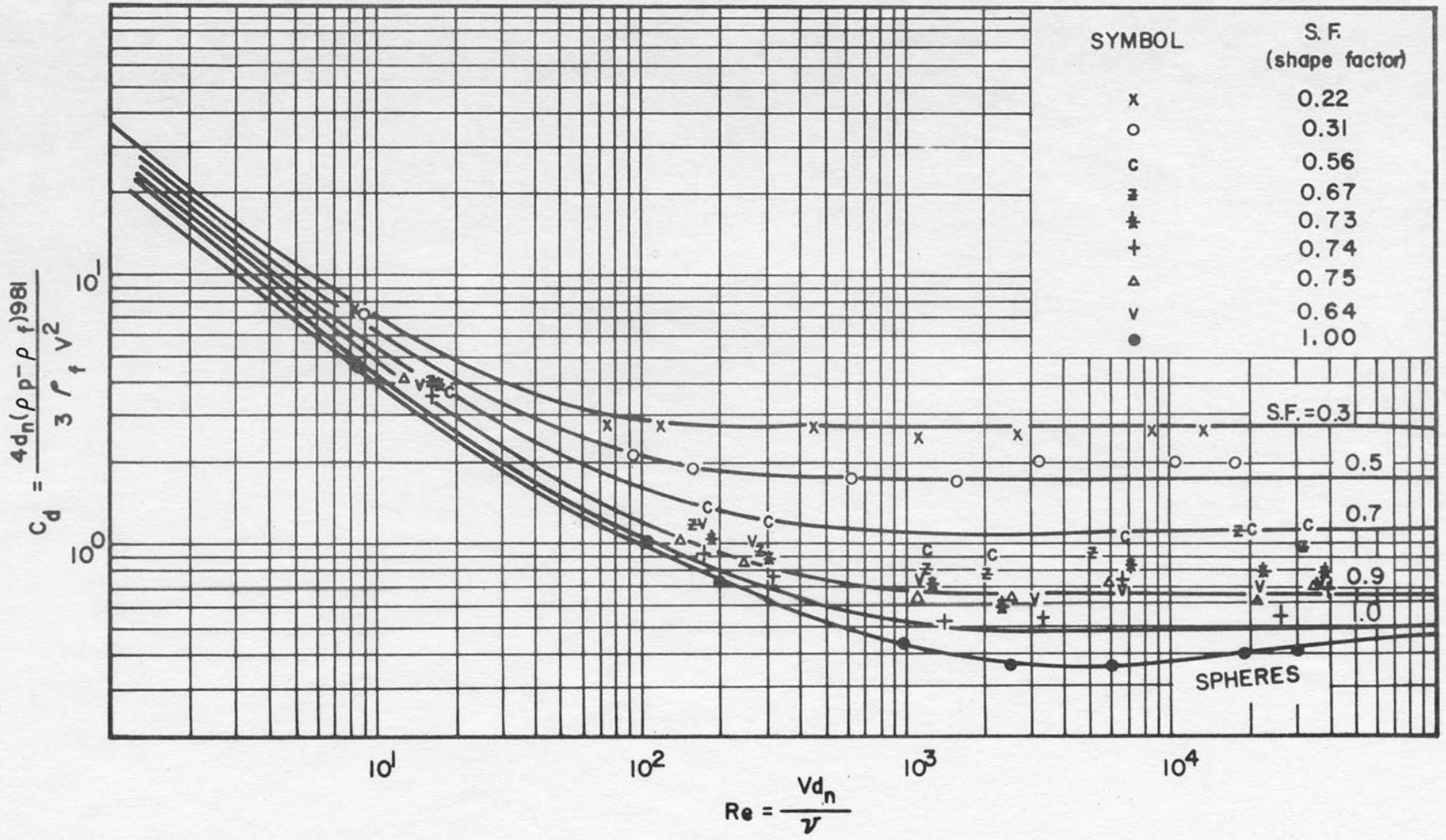


FIG. 12 VARIATION OF DRAG COEFFICIENT WITH REYNOLDS NUMBER AS TAKEN FROM REFERENCE 11

curves as taken from reference 11, however Schulz (9) and Wilde (15) show this dip in their proposed curves as well as a second hump as the Reynolds number is increased.

Figure 13 relates

$C_d = \frac{4}{3}\left(\frac{d_n}{d_A}\right)^2 \frac{d_n(\rho_p-\rho_f)\,981}{\rho_f V^2}$ to $Re = \frac{V d_A}{\nu}$ with S. F. $\left(\frac{d_A}{d_n}\right)$ as the third variable as proposed in the theoretical analysis. If one wishes to use the relation for spheres as a reference, it is apparent that the correction $\left(\frac{d_n}{d_A}\right)^2$ is too extreme since plotted points drop below that of the line for spheres. This relation was formulated on the assumption that $d_A$ would be a better indication of the area term in the drag equation than $d_n$ and the substitution was made accordingly. It should be recognizied here that the area term in the drag equation varies from that of the surface area of the particle for very small Reynolds numbers to that of a cross-sectional area for very large Reynolds numbers and the contribution of shear and pressure to total drag have reversed in their respective orders of magnitude. At this point one should only expect the correction to better define the reaction with different shapes but having the same $d_n$. The points for the sphere are not plotted since $\frac{d_A}{d_n} = 1$ and no change would occur.

In order to provide a similar relation but one in which the sphere curve could still be used as a reference the relation

$C_d = \frac{4}{3}\left(\frac{d_n}{d_A}\right) \frac{d_n(\rho_p-\rho_f)\,981}{\rho_f V^2}$ to $Re = \frac{V d_A}{\nu}$ was plotted in Fig. 14

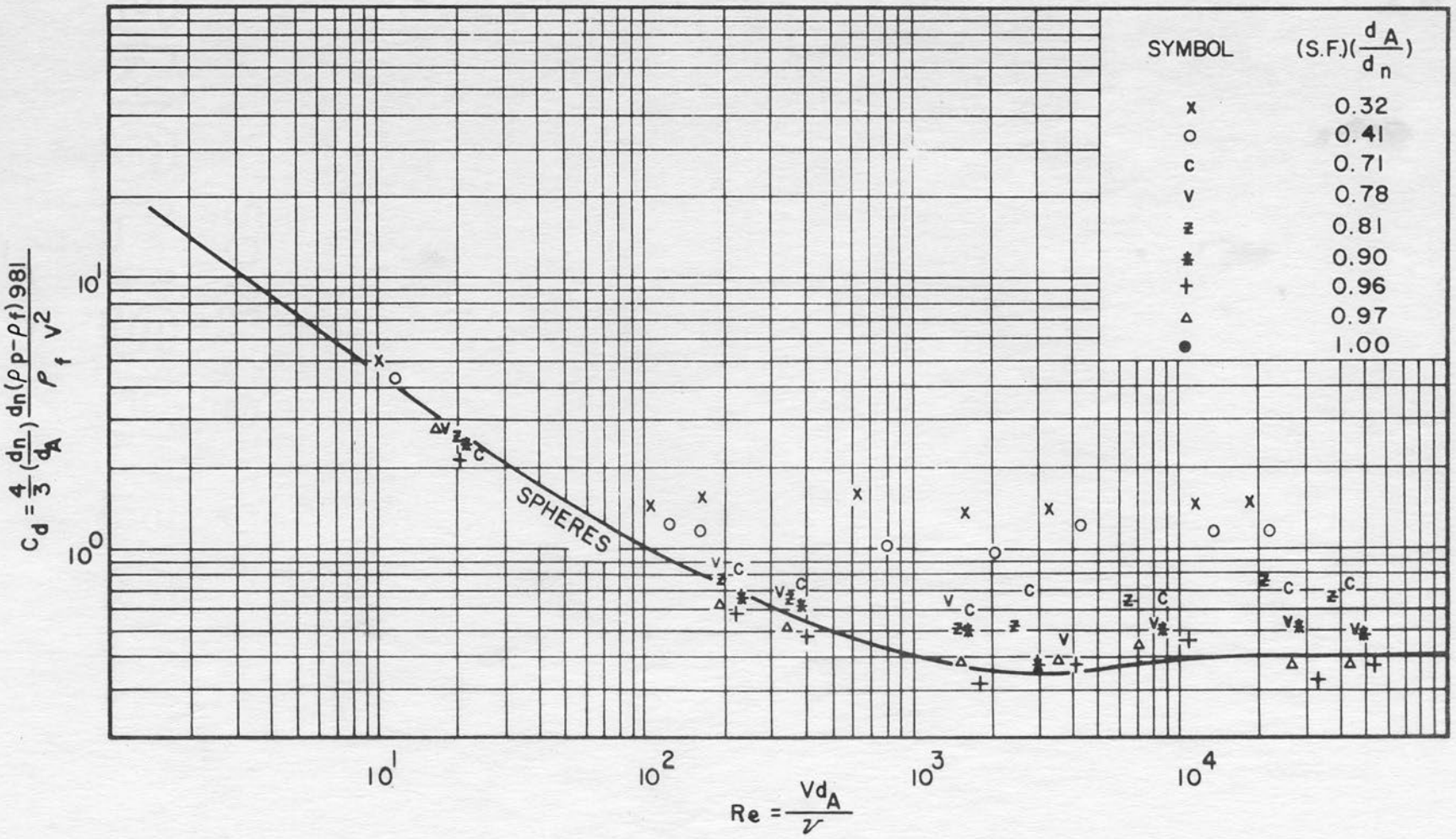


FIG. 13 VARIATION OF DRAG COEFFICIENT WITH REYNOLDS NUMBER USING $(\frac{d_n}{d_A})^2$ AND S.F.$(\frac{d_A}{d_n})$

with the Corey shape factor multiplied by the correction factor $\frac{d_A}{d_n}$ as the third variable. This factor henceforth will be referred to as S. F. $\left(\frac{d_A}{d_n}\right)$

By using the term $\frac{d_n}{d_A}$, all points plot above that of the curve for spheres and approach this relation for low Reynolds numbers. Also, by using the third variable as S. F. $\left(\frac{d_A}{d_n}\right)$, a logical location and orientation is given to the curves representing individual particles. There still is some scatter for the more angular particles and the effect of angularity should be investigated to further refine the results of this work.

A check was made at this point using the machined aluminum shapes. The results of these tests are given in Table III. All particles were dropped in water at 11 degrees centigrade. A superposition of these results (see Table III) on Fig. 14 shows reasonable agreement with the proposed curves.

C. Prediction of Fall Velocity of Larger Particles

A concrete cylinder and the two steel cylinders were used in order to determine if valid predictions of fall velocity could be made from Fig. 14. Since these particles were falling at large Reynolds numbers in the inertial region where $C_d$ becomes independent of the Reynolds number; the predicted velocity could be found from the relationship

$$V = \sqrt{\frac{4}{3}\left(\frac{d_n}{d_A}\right)\frac{d_n(\rho_p-\rho_f)\,981}{\rho_f C_d}}$$ where $C_d$ was taken from Fig. 14

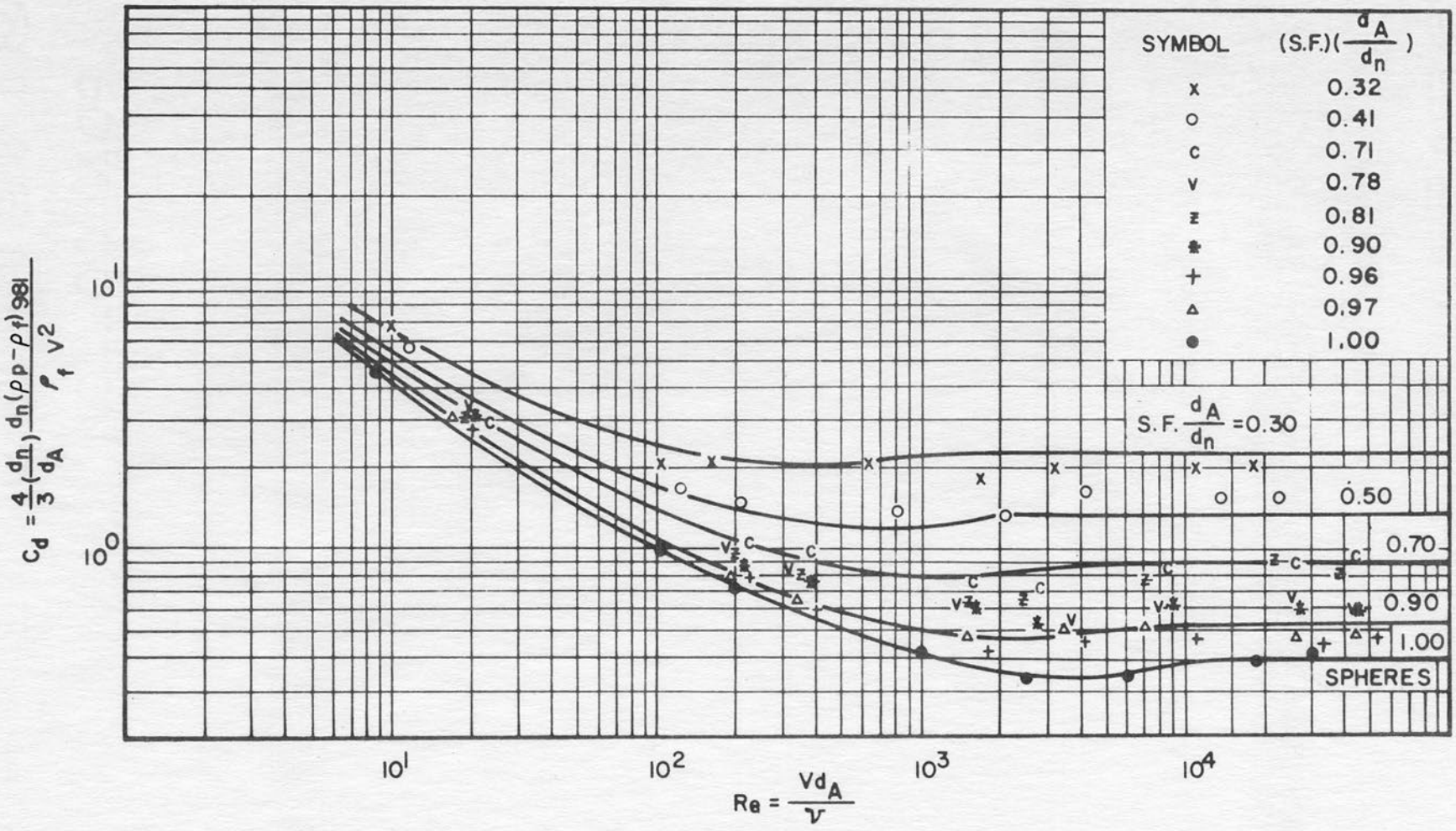


FIG. 14 VARIATION OF DRAG COEFFICIENT WITH REYNOLDS NUMBER USING $\left(\frac{d_n}{d_A}\right)$ AND S.F. $\left(\frac{d_A}{d_n}\right)$

knowing the value of S. F. $\left(\frac{d_A}{d_n}\right)$. The results of the tests and the predicted fall velocities are given in Table V. The measured velocity was computed from an average of the time for the ten drops. These results show a very close agreement between measured and predicted velocities. A comparison using the Corey shape factor and Fig. 12 shows considerable disagreement illustrating the distinct advantage of the new shape parameter which is the third variable in Fig. 14. This comparison with the per cent deviation from the measured velocities is given in Table V. The per cent deviation of the calculated velocities using Fig. 14 and the shape parameter S. F. $\left(\frac{d_A}{d_n}\right)$ are all less than 2 per cent while the deviation using the Corey shape factor ranges from 10 to almost 20 per cent.

In view of the results for the machined shapes and those for the large cylinders, the new shape parameter and drag relationship better describes particle behavior under free fall conditions.

TABLE V

PREDICTED AND MEASURED VELOCITIES OF

LARGE CONCRETE AND STEEL CYLINDERS

| Particle No. | Measured Average Velocity | Predicted Velocity Fig. 14 | Per Cent Deviation | Predicted Velocity Fig. 12 S. F. | Per Cent Deviation |
|---|---|---|---|---|---|
| 17 | cm/sec 220 | cm/sec 218 | 1 | cm/sec 246 | 11 |
| 18 | 204 | 200 | 2 | 177 | 13 |
| 19 | 379 | 372 | 2 | 306 | 19 |

# CHAPTER VI

## SUMMARY AND CONCLUSIONS

A drag - Reynolds number relation has been found for a series of irregular shaped particles up to Reynolds numbers of approximately 400, 000. These relations were determined by dropping each particle in fluids of varying viscosities and measuring the terminal fall velocity.

The irregular shapes used were selected from natural gravel-sized particles and the data collected were supplemented by results of tests with machined aluminum particles and large concrete and steel cylinders.

The photographs of the particles indicate that particles will fall with a quite stable orientation for small Reynolds numbers. However, as the Reynolds number is increased the motion of individual particles may be one or a combination of the several types including tipping, sliding and rotation or some combination of these motors.

In general it is concluded that an increase of the shape parameter S. F. $\left(\frac{d_A}{d_n}\right)$ indicates a decrease in the sliding-tipping motion and an increase in particle rotation.

These various types of motion are influenced to a great extent by separation and the effect of vortex formation on the shear and pressure distribution.

The region in the $C_d$-Re relationship where the drag coefficient becomes independent of the Reynolds number appears to be related to the point at which the separation zones are fully developed.

A new shape parameter is described as S.F. $\left(\frac{d_A}{d_n}\right)$ where S.F. is the Corey shape factor $\frac{c}{\sqrt{ab}}$.

The results obtained from tests with the gravel-sized particles and the supplemental data collected using the larger concrete and steel cylinders to test these results indicate that the fall velocity of larger particles can be accurately predicted. This degree of correlation is not possible using the Corey shape factor.

Various inherent problems became evident during the course of this investigation and their solution would extend the range of knowledge. These problems may be summarized as follows:

1. Cubes in free fall in a viscous fluid can not be described with the three types of motion cited above. Can this behavior be formulated ?

2. What is the effect of roughness and angularity of the particles on the parameter S.F. $\left(\frac{d_A}{d_n}\right)$ ?

3. Is it possible to formulate equations of motion for the various shapes at all Reynolds numbers ?

4. There appears to be a point for each shape at which a certain amount of instability occurs. Can this instability be described and analyzed ?

5. Will an extension of these results for larger particles lead to a sound model law for particles having the same shape factor S.F. $\left(\frac{d_A}{d_n}\right)$ ?

# BIBLIOGRAPHY

## Particle Shape and Fall Velocity


1. Corey, A. T. Influence of shape on the fall velocity of sand grains. Masters Thesis, 1949, Colorado A and M College. 102p. ms.

2. Heywood, H. Measurement of the fineness of powdered materials. Engineering. 146:412-494, 1938.

3. Krumbein, W. C. Measurement and geological significance of shape and roundness of sedimentary particles. Journal of Sedimentary Petrology. 11:64-72, 1941.

4. Malaika, Jamil. Effect of shape of particles on their settling velocity. Ph.D. Dissertation, 1949, State University of Iowa. 64 p. ms.

5. McNown, J. S., Lee, H. M., McPherson, M. B., and Enges, S. M., Influence of boundary proximity on the drag of spheres. Iowa Inst. of Hydraulic Research. Reprint No. 81 from the Proceedings of the VII International Congress for Applied Mechanics, London, 1948. 13p.

6. McNown, J. S., and Malaika, Jamil. Effects of particle shape on settling velocity at low Reynolds numbers. American Geophysical Union. Transactions, 1950. 31:74-82.

7. McPherson, M. B. Boundary influence on the fall velocity of spheres at Reynolds numbers beyond Stokes range. Masters Thesis, State University of Iowa. 39p. ms.

8. Richards, R. H. Velocity of galena and quartz falling in water. American Institute of mining engineers. Transactions. 38:210-235, 1908.

9. Schulz, E. F. Influence of shape factor on the fall velocity of small sand grains. Masters Thesis, 1953, Colorado A and M College. 111p. ms.

10. Serr, E. F. A comparison of the sedimentation diameter and the sieve diameter for various types of natural sands. Masters Thesis, 1948, Colorado A and M College. 82p. ms.

11. U. S. Inter Agency Report No. 12, 1957. Some fundamentals of particle size analysis. U. S. Dept. Army, St. Paul, Minn.

12. Wadell, H. Sphericity and roundness of rock particles. Journal of Geology. 41:310-331, 1933.

13. Wadell, H. The coefficient of resistance as a function of Reynolds number for solids of various shapes. Franklin Institute Journal. 217: No. 4:459-490, 1934.

14. Wadell, H. Volume, space, and roundness of rock particles. Journal of Geology. 40:443-451, 1932.

15. Wilde, R. H. Effect of shape on the fall velocity of gravel-sized particles. Masters Thesis, 1952, Colorado A and M College. 86p. ms.

16. Zegrzda, A. P. Settling of gravel and sand in water. Leningrad. Nauchno - Issledouatelskouo. 12:30-54, 1934. English Translation: In appendix of "Influence of Shape on the Fall Velocity of Sedimentary Particles", by E. F. Schulz, R. H. Wilde, and M. L. Albertson. Report No. 53-10. May, 1953. Colorado A and M. College, Department of Civil Eng.

Fine Material Concentration

17. Chakravarti, S. K. Studies of the electrochemical, viscometric and swelling characteristics of pure clay minerals and their mixtures. Indian Society of Soil Science Journal. 6:239-246, 1958.

18. Grim, R. E. Ion exchange in relation to some properties of soil-water systems. In Symposium on Exchange Phenomena in Soils. 55th Annual Meeting, A. S. T. M., N. Y., N. Y. June 27, 1952. A. S. T. M. special publication No. 142. p.3-9.

19. Hubbel, D. W., and Khalid al-Shaikh Ali. Flume studies of the effect of temperature on the mechanics of flow in alluvial channels. U.S.G.S. in press. Chpt. F, March, 1962. CER61DWH68.

20. Riddick, T. M. Zeta potential and its application to difficult waters. American Water Works Association Journal. 53:1007-1030.

21. Rogers, W. F. Composition and properties of oil well drilling fluids. Gulf Publishing Co., Houston, Texas. p.112, 268, 1953.

22. Simons, D. B., Richardson, E. V., and Haushild, W. L. Some properties water-clay dispersions and their effects on flow. U.S.G.S. in press. Studies of flow in alluvial channels. Aug., 1961. CER61DBS50.

23. Street, Norman. Viscosity of clay suspensions. World Oil. 147:151-156, 1958.

24. Wood, W. H., Granquist, W. T., and Krieger, I. M. Viscosity studies on dilute clay mineral suspensions. Clays and Minerals. Nat'l Research Council Publ. 456. p.240-250.

25. Yotsukura, Nobuhiro. Effect of Bentonite suspension on sand transport in four-inch pipe. Ph.D. Dissertation, 1961, Colorado State University. 184 p.

Textbooks

26. Albertson, M. L., Barton, J. R., and Simons, D. B. Fluid mechanics for engineers., Prentice Hall, N.J., 1960. 561 p.

27. Baver, L. D. Soil physics. 3d ed. John Wiley and Sons, Inc., New York, 1956. 489 p.

28. Bingham, E. C. Fluidity and plasticity. McGraw-Hill Book Co., New York, 1922. 440 p.

29. Eirich, F. R. Rheology. Academic Press, Inc., New York, Vol.3, 1956.

30. Goldstein, S. Modern developments in fluid mechanics. Oxford Press, London, Vol. 1 and 2, 1938. 702 p.

31. Lamb, Sir Horace. Hydrodynamics. Dover Publications. New York, 1945. 738 p.

32. Rouse, H. Elementary mechanics of fluids. New York, John Wiley and Sons. 1946. 376 p.

33. Schlicting, H. Boundary layer theory. McGraw-Hill Book Co., New York, 1955. 535 p.

34. Vallentine, H. R. Applied hydrodynamics. Butterworths Scientific Publications. London, 1959. 272 p.

## Particle Motion

35. Willmarth, W. W., Hawk, N. E., and Harvey, R. L. Steady and unsteady motions and wakes of freely falling disks. The Physics of Fluids. Vol. 7, No. 2, February, 1964. p. 197-208.

# APPENDIX (A) SUMMARY OF DATA

TABLE VI

PARTICLES IN 100% GLYCERINE

| Particle No. | Terminal Fall Velocity (cm/sec) | $C_d$ | Re | Temp°C |
|---|---|---|---|---|
| 1 | 25.2 | 4.79 | 8.84 | 23.2 |
| 2 | 21.4 | 6.79 | 10.0 | 23.2 |
| 3 | 24.4 | 5.78 | 11.8 | 23.2 |
| 4 | 35.2 | 2.83 | 20.8 | 23.2 |
| 5 | 31.7 | 3.16 | 17.4 | 23.2 |
| 6 | 37.4 | 3.14 | 19.9 | 23.2 |
| 7 | 40.2 | 2.91 | 23.7 | 23.2 |
| 9 | 33.8 | 3.30 | 18.5 | 23.2 |
| 10 | 36.1 | 2.89 | 20.9 | 23.2 |

TABLE VII

PARTICLES IN 90% GLYCERINE, 10% WATER (VOLUME)

| Particle No. | Terminal Fall Velocity (cm/sec) | $C_d$ | Re | Temp°C |
|---|---|---|---|---|
| 1 | 55.0 | 1.08 | 107 | 23.2 |
| 2 | 40.1 | 1.98 | 104 | 23.2 |
| 3 | 46.1 | 1.66 | 123 | 23.2 |
| 4 | 68.5 | 0.77 | 225 | 23.2 |
| 5 | 63.2 | 0.83 | 191 | 23.2 |
| 6 | 67.6 | 0.99 | 200 | 23.2 |
| 7 | 67.1 | 1.08 | 220 | 23.2 |
| 9 | 62.3 | 1.01 | 188 | 23.2 |
| 10 | 70.0 | 0.79 | 225 | 23.2 |

TABLE VIII

PARTICLES IN 85% GLYCERINE, 15% WATER (VOLUME)

| Particle No. | Terminal Fall Velocity (cm/sec) | $C_d$ | Re | Temp°C |
|---|---|---|---|---|
| 1 | 67.1 | 0.74 | 208 | 24.5 |
| 2 | 39.4 | 2.09 | 164 | 24.5 |
| 3 | 48.8 | 1.49 | 210 | 24.5 |
| 4 | 77.7 | 0.61 | 408 | 24.5 |
| 5 | 71.5 | 0.66 | 347 | 24.5 |
| 6 | 75.3 | 0.81 | 355 | 24.5 |
| 7 | 71.9 | 0.95 | 378 | 24.5 |
| 9 | 69.0 | 0.84 | 335 | 24.5 |
| 10 | 73.4 | 0.73 | 378 | 24.5 |

TABLE IX

PARTICLES IN 70% GLYCERINE, 30% WATER (VOLUME)

| Particle No. | Terminal Fall Velocity (cm/sec) | $C_d$ | Re | Temp°C |
|---|---|---|---|---|
| 1 | 88.7 | 0.44 | 1000 | 22.5 |
| 2 | 42.0 | 2.10 | 639 | 22.5 |
| 3 | 51.5 | 1.41 | 806 | 22.5 |
| 4 | 94.3 | 0.43 | 1810 | 22.5 |
| 5 | 85.0 | 0.49 | 1510 | 22.5 |
| 6 | 85.9 | 0.65 | 1490 | 22.5 |
| 7 | 81.2 | 0.77 | 1560 | 22.5 |
| 9 | 80.1 | 0.65 | 1420 | 22.5 |
| 10 | 81.3 | 0.62 | 1520 | 22.5 |

TABLE X

PARTICLES IN 55% GLYCERINE, 45% WATER (VOLUME)

| Particle No. | Terminal Fall Velocity (cm/sec) | $C_d$ | Re | Temp$^0$C |
|---|---|---|---|---|
| 1 | 99.0 | 0.38 | 2620 | 19 |
| 2 | 44.8 | 1.79 | 1590 | 19 |
| 3 | 55.5 | 1.30 | 2020 | 19 |
| 4 | 95.3 | 0.46 | 4250 | 19 |
| 5 | 86.1 | 0.51 | 3550 | 19 |
| 6 | 88.5 | 0.65 | 2480 | 13.5 |
| 7 | 87.6 | 0.71 | 2730 | 19 |
| 9 | 92.6 | 0.52 | 3820 | 19 |
| 10 | 96.0 | 0.48 | 2920 | 13.5 |

TABLE XI

PARTICLES IN 40% GLYCERINE, 60% WATER (VOLUME)

| Particle No. | Terminal Fall Velocity (cm/sec) | $C_d$ | Re | Temp$^0$C |
|---|---|---|---|---|
| 1 | 103.0 | 0.37 | 6250 | 20 |
| 2 | 45.4 | 1.92 | 3260 | 15 |
| 3 | 50.5 | 1.66 | 4230 | 20 |
| 4 | 98.0 | 0.46 | 11000 | 22.5 |
| 5 | 82.4 | 0.51 | 7170 | 15 |
| 6 | 81.5 | 0.81 | 6410 | 20 |
| 7 | 82.5 | 0.84 | 8450 | 20 |
| 9 | 86.5 | 0.63 | 8190 | 20 |
| 10 | 85.0 | 0.65 | 8530 | 20 |

TABLE XII

PARTICLES IN WATER AT 8°C

| Particle No. | Terminal Fall Velocity (cm/sec) | $C_d$ | Re | Temp°C |
|---|---|---|---|---|
| 1 | 109 | 0.41 | 19,400 | 8 |
| 2 | 47.7 | 1.98 | 11,300 | 8 |
| 3 | 55.6 | 1.55 | 13,600 | 8 |
| 4 | 111 | 0.43 | 33,300 | 8 |
| 5 | 99.0 | 0.49 | 27,400 | 8 |
| 6 | 81.5 | 0.97 | 22,000 | 8 |
| 7 | 86.5 | 0.91 | 25,900 | 8 |
| 9 | 95.0 | 0.63 | 26,300 | 8 |
| 10 | 94.0 | 0.63 | 27,600 | 8 |

TABLE XIII

PARTICLES IN WATER AT 27°C

| Particle No. | Terminal Fall Velocity (cm/sec) | $C_d$ | Re | Temp°C |
|---|---|---|---|---|
| 1 | 109 | 0.41 | 32,000 | 27 |
| 2 | 47.5 | 1.99 | 18,350 | 27 |
| 3 | 56.4 | 1.57 | 22,500 | 27 |
| 4 | 106 | 0.47 | 51,900 | 27 |
| 5 | 101 | 0.47 | 45,500 | 27 |
| 6 | 88.7 | 0.81 | 38,900 | 27 |
| 7 | 84.6 | 0.95 | 41,400 | 27 |
| 9 | 97.7 | 0.60 | 45,200 | 27 |
| 10 | 97.8 | 0.59 | 47,500 | 27 |

# APPENDIX (B) APPARENT VISCOSITY

# APPARENT VISCOSITY

This study was conducted as an auxiliary study to that of the main topic of fall velocity and surface area. A condensed presentation and discussion follow in the remaining pages.

Beginning with the equations by Einstein and proceeding through the various later developments with reference to viscosity of suspensions, one sees that the viscosity of the suspension relates primarily to only the volume of the suspended solids and to the configuration of the conglomeration of suspended particles. However, in recent years other investigators have shown that particle charge and the diffuse double layer affect the degree of hydration and in turn the viscosity of the suspensions.

At this point it appears that if one wishes to know the effect of a concentration of fine material on the apparent viscosity of a solution, he must recognize both particle volume and particle charge. The investigations made as part of this dissertation are only intended to indicate the interdependency of these variables for a complete understanding of apparent viscosity effects.

## A. Components of the Equipment

1. Fall Column - The fall column consisted of a plastic tube, four feet long and six inches in diameter. The bottom of the tube was sealed with a plexiglass plate inserted with a one-inch diameter plastic tube at the center line. On the end of the one-inch tube was placed a

short piece of plastic hose with a pinch clamp. This whole system was held in a vertical position by means of a pipe stand (see figure 15). The base of the stand was provided with four bolts in order to plumb the tube. Figure 15 also shows a cloud of fine material in suspension in the fall column.

2. Accessories - The time of fall between two fixed points in the fall column was measured to hundredths of a second using a stop watch. A centigrade thermometer was used to measure temperature. Thin straight wires were supported six inches in front of the fall column at the two fixed points. Sighting between a wire and a fixed mark on the fall column eliminated any parallax that could have been encountered. The average time for five successive drops was used for computations of fall velocity.

B. Particle Properties

Two types of particles were used to form the concentration of fine material for these tests. One type consisted of very fine plastic beads (Vestyron type N). These beads had an average density of 1.05 grams per cubic centimeter and were of varying diameter but less than 0.046 inches. The beads were sieved into two size groups, those passing the 0.046-inch sieve and retained on a 0.0276-inch sieve, and those passing a 0.0232-inch sieve and retained on the pan. The second type also possessed an average density of 1.05 grams per cubic centimeter but were larger in size and of a cylindrical shape. The major axis averaged

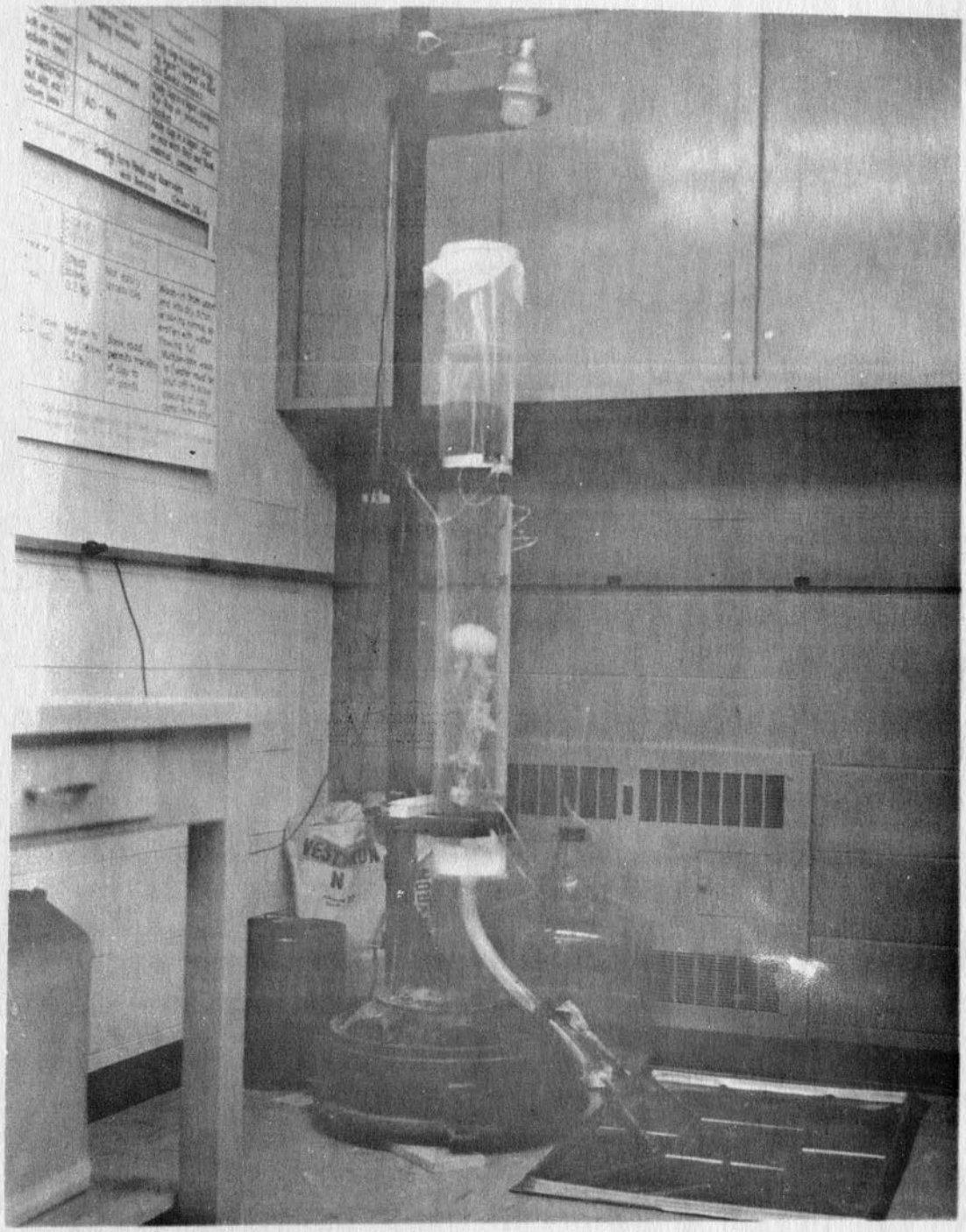

FIG. 15 DROP APPARATUS FOR FINE MATERIAL CONCENTRATION STUDY

0.3 centimeters, the intermediate 0.3 centimeters, and the minor, 0.2 centimeters, see Fig. 16.

The sphere which was dropped through the suspension was red in color; had a density of 1.152 grams per cubic centimeter and a diameter of 1.268 centimeters. This sphere was also of a plastic material.

C. Fluids

The fluid used for these tests was formed by adding a commercial salt to water until a density of 1.042 grams per cubic centimeter was created. This density gave the best results and held the fine particles suspended in the salt solution for several hours.

D. Procedure

With the fall column properly positioned and filled with salt water, a series of five drops with one particle was made in the clear salt solution in order to obtain the velocity (V'). The particle was released by hand just under the surface of the solution and timed using the stop watch as it fell between two points located 71.1 centimeters apart. A bulk volume of 400 cubic centimeters of fine particles was added and the process continued until the desired range of concentrations was achieved. High wattage lights were placed behind the fall column opposite the observer at the end points of the fixed distance. This enabled the observer to see the particle as it fell through the concentration of suspended fine material.

Drops were made in several of the concentrations as well as in

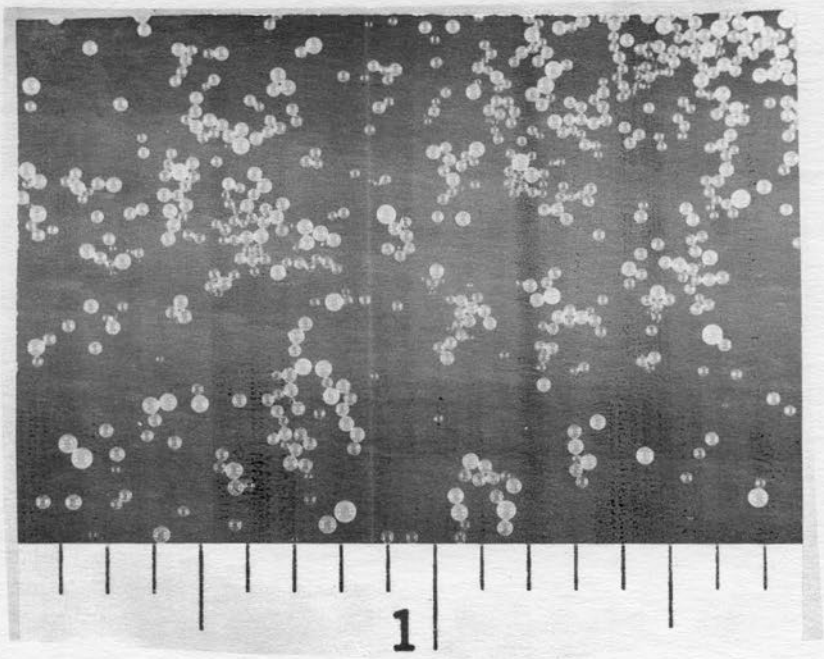

FINE PLASTIC BEADS (VESTYRON)

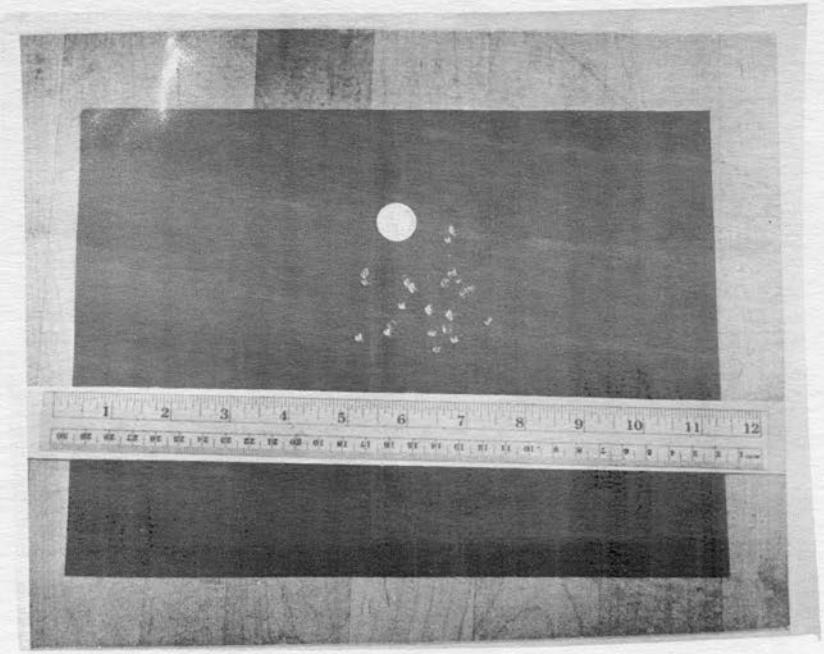

CYLINDRICAL GRANULATE (VESTYRON)

FIG. 16. PHOTOGRAPHS OF FINE PLASTIC BEADS AND CYLINDRICAL GRANULATE USED TO FORM NEUTRALLY BUOYANT SOLUTIONS

the clear salt solution at various temperatures. This was done in order to correct the observed fall velocities to a standard temperature.

E. Discussion of Results

The fall velocities obtained from the tests made with the neutrally buoyant particles and a heavier, plastic sphere indicate that particle volume alone does not adequately describe the apparent viscosity effect as some earlier investigators had surmised.

The results of the various tests are plotted in figure 17 in order to show the effect of the volume concentrations of neutrally buoyant particles on the fall velocity of a heavier particle. The ratio of $\frac{Vc}{V'}$ versus concentration of fines by volume indicates the effects of particle charge. $V'$ is the fall velocity of a plastic sphere ($\rho_p = 1.152$ gm/cc) of diameter 1.268 centimeter in the clear salt solution at $20^0$ centigrade. Vc is the fall velocity of the same sphere in a given concentration of neutrally buoyant fine material. Vc in the plot has been corrected to 20 degrees centigrade for all points shown.

The two sizes of spherical particles follow almost identical paths showing a decrease in the ratio of $\frac{Vc}{V'}$ or an increase of apparent viscosity up to about 5.5 percent concentration and then an increase in $\frac{Vc}{V'}$ (decrease in apparent viscosity) up to a concentration of 6.5 percent and then a further decrease.

At 6.5 percent, the ratio of $\frac{Vc}{V'}$ has returned to 1.00 or in other words, the plastic sphere is falling at the same speed in the 6.5

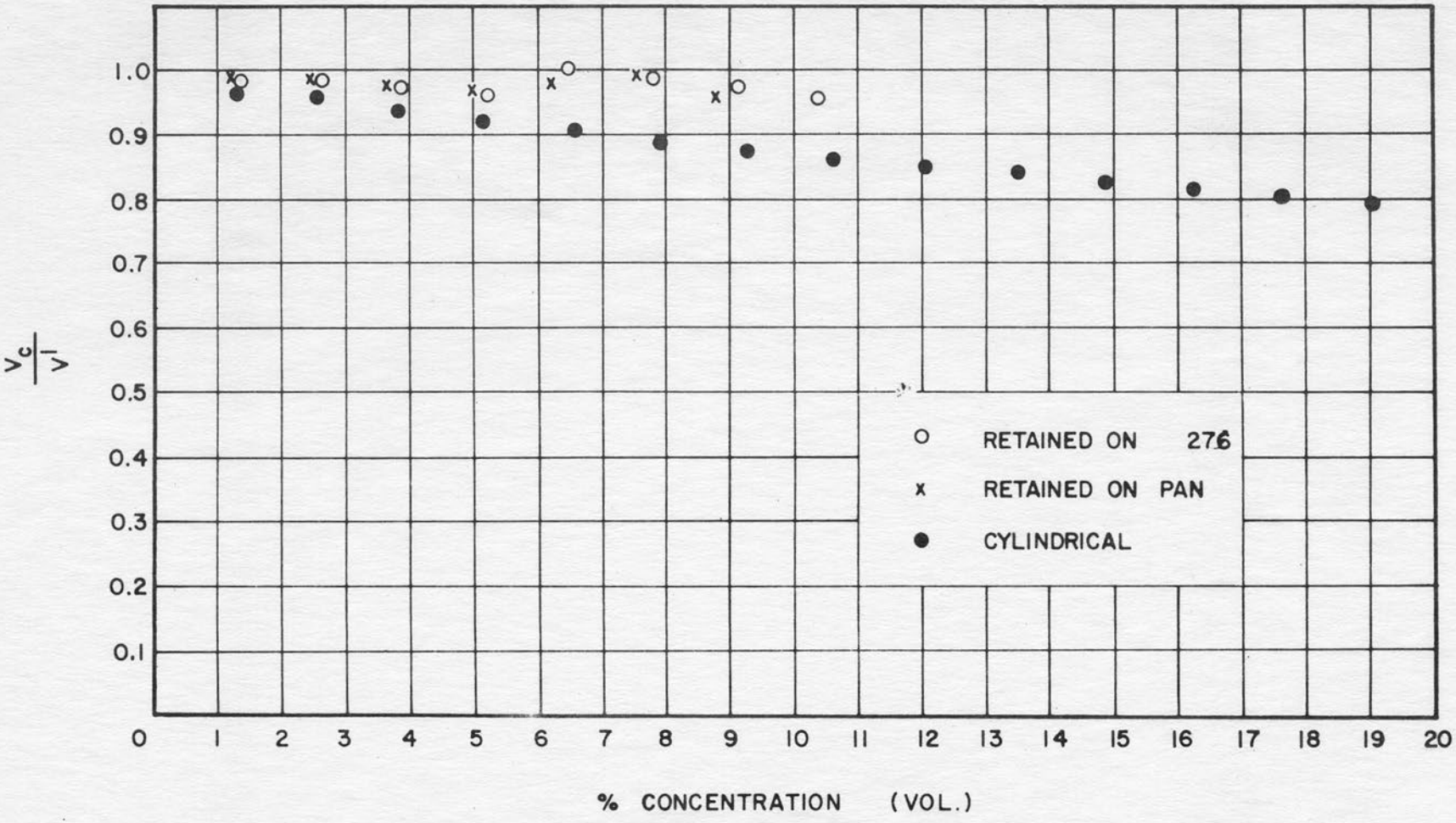


FIG. 17 VARIATION OF RELATIVE VELOCITY WITH PERCENT CONCENTRATION OF NEUTRALLY BUOYANT FINE MATERIAL FOR A FALLING SPHERE

percent concentration as it did at zero concentration and the apparent viscosities appear to be the same for zero and 6.5 percent concentration.

In contrast the larger cylindrical particles do not exhibit this property but show a continual decrease in $\frac{Vc}{V'}$ (increase in apparent viscosity) with increasing concentration.

The explanation for this might be considered in the following manner. The small spherical particles exhibit a large electrostatic charge and will not disperse in water. However, when placed in the salt solution (about 1.3 normal) they exhibit complete dispersion. Unfortunately, the necessary equipment was not available for the measurement of zeta potential.

A test for the cation exchange showed 9 milli. equiv./100 grams. This may appear low in comparison with the cation exchange capacity of bentonite clays, but on the other hand, the surface area exposed per 100 grams for the plastic beads is much less than that per 100 grams of clay; thus, the charge per unit of surface area on the beads is very high. The fact that the beads disperse in the salt solution and not in water indicates an ion exchange with possible replacement by sodium. The fixation of the sodium ion on the beads results in a change in the character of the initial medium. This would take place to varying degrees as more beads are added as opposed to the availability of the sodium ion at that particular stage.

The curves shown in Chakravarti's (17) work tend to indicate

what may be happening with the change in added base due to the fixation of the sodium ions. A reproduction of some of these curves is shown in figure 18. From these curves it appears that the apparent viscosity is changing due to the physical volume of fines present and also to the particle charge.

The larger cylindrical particles did not exhibit this large electrostatic charge and being more inert in this respect, did not behave in the same manner. These appeared only to effect apparent viscosity by change in volume.

It should be noted, of course, that at the same time the charge per unit surface area on the large particles had decreased the effective weight had increased and in this respect the relative role of particle charge and weight were different from that of the finer material.

The limit in the range of concentrations covered was due to the fact that one could no longer see the larger sphere falling through the higher concentration of fines.

F. Conclusions

The work done on fall velocity as affected by neutrally buoyant fine material indicates the need for the development of some special instrumentation and measuring techniques. There is a good possibility that sensitive pressure transducers might be used to indicate the falling sphere as it passes a particular point in a fall column. The effect on fall velocity for varying concentration of clay suspensions could then be

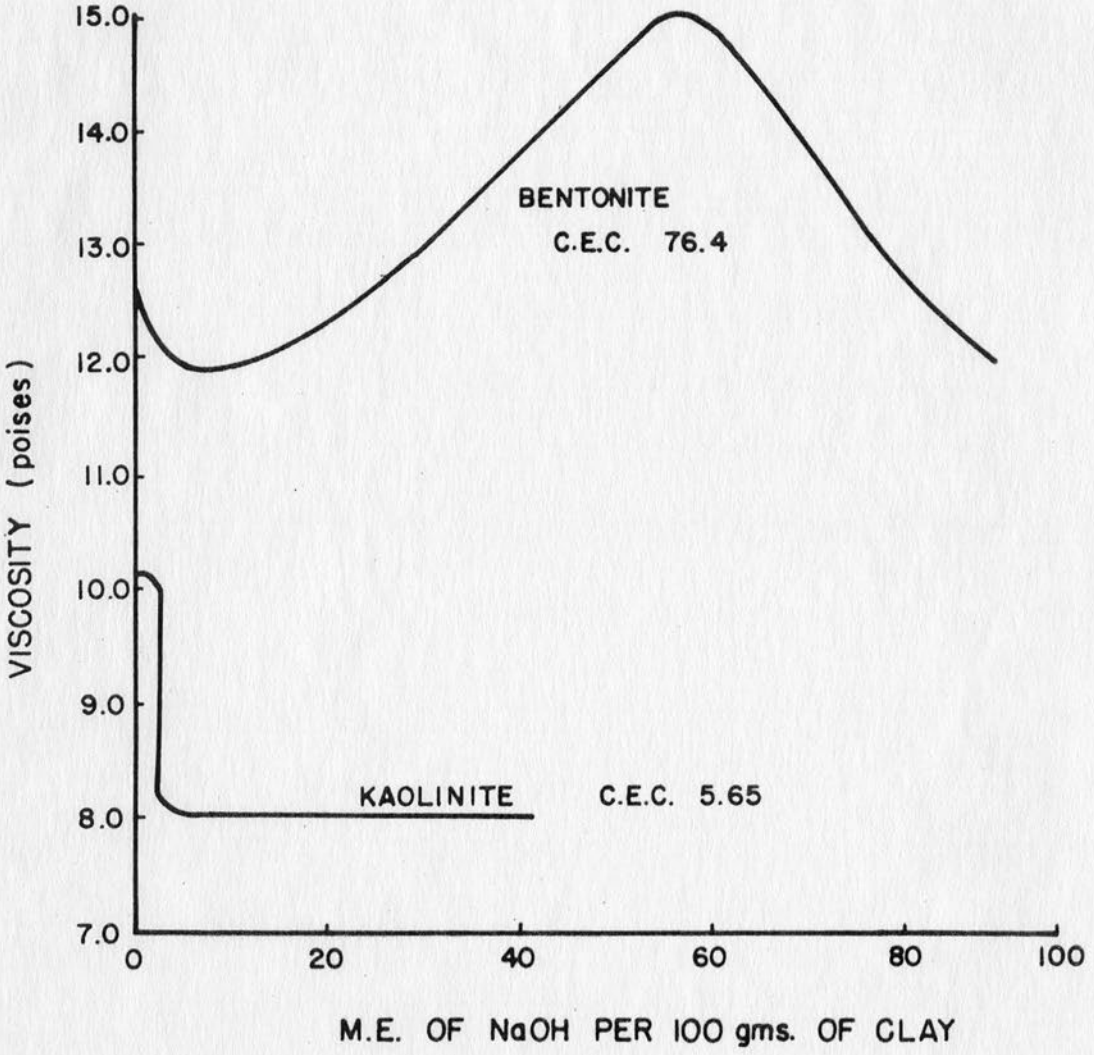


FIG. 18 VARIATION OF VISCOSITY OF CLAY SUSPENSIONS WITH ADDED BASE (AFTER CHAKRAVARTI)

formulated. It is apparent from the results that for the clay size fraction of suspended fine material attention should be given to particle charge as well as volume concentration as they affect apparent viscosity. If the type of fine material present is highly charged, this charge could materially affect apparent viscosity and in turn fall velocity.

Zeta potential would appear to be one parameter that would be indicative of particle charge and which could possibly lead to formulations dealing with both volume concentration and particle charge. Attention should also be given to effect of adding a dispersing agent to fine material in suspension as it in turn will effect the apparent viscosity of the resulting suspension as well as the effect due to the volume concentration. This study points to the need for further research into the effects of fine material concentration on the fall velocity of larger sizes.